FACULTY OF SCIENCE AND TECHNOLOGY
MASTER'S THESIS

Study programme / specialisation: MSc. Petroleum Geoscience Engineering	The spring semester, 2023 Open / Confidential
Author: Kelvin Nana Nuamah Wireko	
Supervisor at UiS: Wiktor Waldermar Weibull Co-supervisor: Thomas Meldahl Olsen External supervisor(s):	
Thesis title: 3D Processing, Imaging and Interpretation of Dense Sub Bottom Profile Data Acquired in Avaldsnes and Hafrsfjord	
Credits (ECTS): 30	
Keywords: seismic processing, seismic imaging, seismic interpretation, sub bottom profiling, shallow water environment, nearshore environment	Pages: 67 Stavanger, June, 14, 2023

Acknowledgements

I would like to take this opportunity to express my deepest gratitude and appreciation to the individuals who have supported me throughout the journey of completing this thesis. Their unwavering encouragement, love, and understanding have been instrumental in my success. First and foremost, I am immensely grateful to my family. To my parents, Joseph Kofi Wireko and Ruth Daisy Wireko, who have been my pillars of strength and my constant source of motivation. Your belief in me, your sacrifices, and your endless support have been invaluable. I am eternally grateful for the opportunities you have provided me and for instilling in me the importance of education and hard work. I would also like to extend my heartfelt thanks to my siblings, Philip Wireko and Daisy Wireko. I am indebted to my supervisors, Wiktor Waldermar Weibull and Thomas Meldahl Olsen, for their guidance, expertise, and patience throughout the research process. Their insightful feedback, constructive criticism, and invaluable advice have significantly contributed to the development and quality of this thesis.

Abstract

This thesis addresses the challenges associated with conducting archaeological seismic surveys in shallow water and nearshore environments, focusing on the effects of dynamic elements such as wind, tide, and waves. These environments are known to contain a wealth of submerged archaeological remains, yet they are often overlooked due to the difficulties posed by their dynamic nature. While seismic geophysical methods are the preferred approach for archaeological prospection and investigations, the presence of dynamic elements hinders the acquisition of data in a regular grid pattern. The methodology employed to tackle these challenges involves creating a 3D grid of various sizes, tidal correction, interpolation and migration of the seismic dataset using the 3D grid. The proposed methodology was tested in Avaldsnes and Hafrsfjord - historically significant areas in Norway known to have shipwrecks. These locations serve as ideal test sites for evaluating the effectiveness of the methodology in addressing the problems posed by dynamic elements in shallow water and nearshore environments. Three 3D grid sizes were tested – 0.1 by 0.1 m, 0.25 by 0.25 m and 0.5 by 0.5 m - and two interpolation methods – cubic and Shepard's interpolation – were tested. Results showed 0.1 by 0.1 m 3D grid size interpolated with Shepard's method and migrated after showed the best seismic image and detail making identifying the shipwreck straightforward. The overall conclusion is that a 3D grid with small sizes, preferably 0.25 by 0.25 m or less, interpolated with Shepard's method show the best seismic image for interpretation eliminating most of the problems caused by dynamic elements.

Contents

Introduction

An increasing number of shipwrecks and other submerged archaeological remains increases the demand for effective subsurface geophysical prospection methods (Wilken et al., 2019). Furthermore, shallow water environments are dynamic areas prone to wind, waves and strong tides, and are rarely investigated in a structured way, unfortunately, because land-sea transitions areas are known to be rich in archaeology remains (Missiaen et al., 2018). Out of all the geophysical prospection methods (gravity, magnetic, electrical, seismic and radiometric). Acoustic geophysical method is the most preferred for archaeological prospection and investigations. Acoustic surveys have been done in a regular grid but the presence of dynamic elements (wind, tide and waves) in nearshore environments prevent a regular grid seismic survey acquisition. Dynamic elements – wind and waves – hinders the boat to produce a regular grid, instead creating a zig-zag pattern and the rise and fall of tides affect the travel time and change the seismic wave travel paths. Previous research acknowledges how dynamic elements (wind, tide and waves) in nearshore environments affect the acoustic survey (Baradello & Carcione, 2008). However, no effective methodology has been created to take into consideration these dynamic elements in seismic imaging and interpretation. Therefore, the effect of dynamic elements in nearshore environments on acoustic data acquisition from a regular grid to an irregular grid and the effect of tides on water depths on seismic migration of high frequency data of partially buried or buried archaeological artifacts is an important research question. Tidal correction, interpolation and migration of the seismic dataset onto a regular grid are the methodology undertaken to tackle the problem of an irregular grid created by dynamic elements. In this thesis, a methodology for processing and imaging 3D zero-offset high frequency seismic data from an irregular set of points is derived. The methodology consists of a series of steps, including statics based tidal correction, binning, with median statistical averaging, interpolation/regularization and seismic migration. The methodology is tested on two datasets acquired in two field sites. The locations are Avaldsnes and Hafrsfjord in Norway. Both are historically important areas with known shipwrecks. This makes them excellent places to test the developed methodology. The two areas pose different challenges to seismic imaging. In Hafrsfjord, the shipwreck (figure 1) lies in an area approximately 42 meters of water depth, while in Avaldsnes the shipwreck lies in an area with less than 1 meter water depth. This thesis seeks to solve the problems created when conducing an archaeological seismic survey in these highly different water depth environments. The objectives of the thesis are: i) Test various interpolation methods for interpolating an irregular dataset to a regular dataset ii) Investigate the optimal interpolation

techniques on two different water depth environments ii) Assess the quality from the interpolation and migration.

Figure 1 3D image of Hafrsford shipwreck (Tywoky, 2022)

Literature Review

A 3D reconstruction of a shallow archaeological site of the Grace Dieu in Hamble River, UK (Plets et al., 2008) was done using a single channel receiver array consisting of a group of eight hydrophones. The Grace Dieu is buried within intertidal muddy sediments and covered by 2 -5 m of water. The main objective of the study was to demonstrate the effectiveness of sub bottom system in detecting shallowly buried objects in very shallow water. The Grace Dieu is known to be fourth and last great ship built for Henry V. The Grace Dieu was the largest vessel ever built in England, up to that time, but unfortunately never saw action. In 1439, the ship was struck by lighting and sunk to the bottom of the Hamble River. In this process of seismic acquisition, two problems were encountered in the survey: One was related to the acoustic source towed behind the motorised vessel and the other was related to the hydrophone unit offset approximately 2m behind the source. Towing the acoustic source

behind a motorised vessel created bubbles from the propellers of the vessel, resulting in an extensive acoustic blanking in the dataset. Secondly, the angle of incidence and reflected ray increases with water depth. Therefore, it can be no longer assumed the angle of incidence is normal in very shallow water. These problems were solved by using a non-motorised deployment and mounting the hydrophone adjacent to the source respectively. From their results as shown in figure 2, the buried wooden haul of the Grace Dieu was imaged successfully and took note that the highly reflective and attenuating nature of degraded wood is a major aid in locating buried shipwreck.

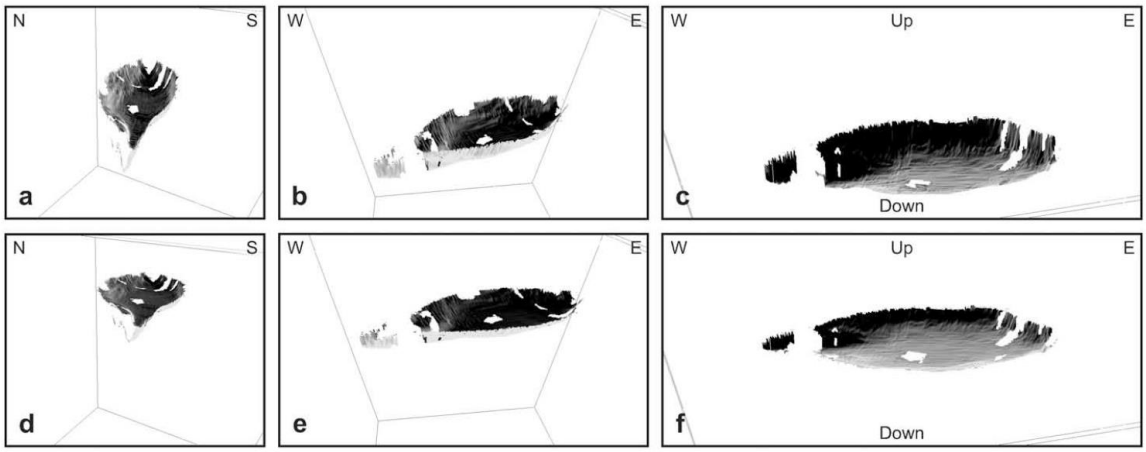

Figure 2 3D reconstruction of the Grace Dieu (Plets et al., 2008)

Wilken et., 2019 did a study on Imaging a medieval shipwreck with the Pinpong 3D marine reflection seismic system. The Pinpong system consists of two piezoelectric sources, six hydrophones and two real -time differential global positioning systems (RTK – DGPS), installed on a buoyant semi-rigid frame. Conducting geophysical investigations for archaeological research requires one to work at the edge of high salinity waterbodies with a depth of few decimetres to metres. Most prospecting methods suffer from high signal attenuation. The design of the Pinpong system works well in stillwater and depths as shallow as 0.3m. However, wave motion cannot be resolved with the system and has to be done through basic residual static correction. The targeted shipwreck for the study was a twelfth century Scandinavian shipwreck located 2 km northwest of the Baltic fjord Schlei, Germany. From their results, the Pinpong system was able to create a data cube with a resolution of 0.15m in all three dimensions which allowed for the targeted ship to be clearly observed. In figure 3, the depth slices show major shipwreck reflections. However, the required horizontal resolution was not achieved in parts of the dataset. This was known because isolated small parts of the ship discovered by divers couldn't be correlated with the seismic reflections.

Some reasons could be: data gaps, not fully suppressed wave noise or the motion of the acoustic sources due to waves resulting in a change in radiation direction.

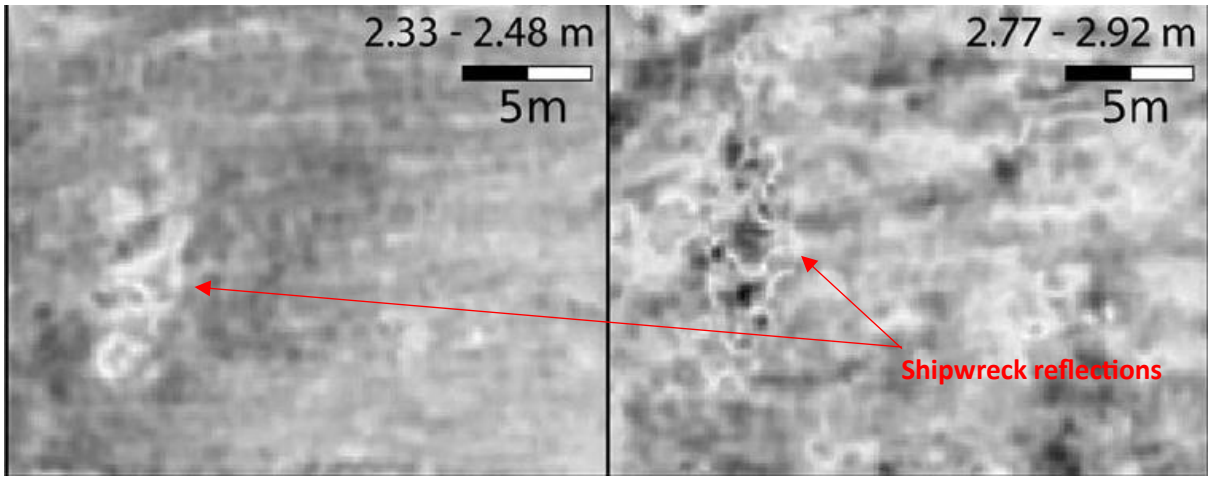

Figure 3 Depth slices of the data cube showing the major reflections of the shipwreck (Wilken et al., 2019)

Another study, Chirping for Large-Scale Maritime Archaeological Survey: A Strategy Developed from a Practical Experience-Based Approach (Grøn & Boldreel, 2014), demonstrated the use of sub-bottom profilers to produce archaeological results. This study was done to demonstrate the cost-effective strategy for large scale mapping of submerged archaeological elements embedded in the sea floor. Optimal detection of submerged archaeological features requires the boat to sail slower, and tune the instrument to achieve maximum horizontal and vertical resolution. In the seismic survey acquisition, different intervals between the survey lines were employed. From this survey, it was found that different intervals between survey lines should be determined by the size and shape of the features being sought. Chirp systems were found to have an advantage over conventional sub-bottom profilers – where conventional refers to sparkers, boomers and parametric systems - in the detection and mapping of shipwrecks embedded in sea floor sediments (Grøn et al., 2015). In Grøn et al. (2015) chirp based acoustic high-resolution sub-bottom profilers were used to detect several wreck parts embedded in sea-floor sediments. The main targets for the study were Akko 4, the late Renaissance wreck Lundeborg 1, Medieval barge Haithabu 4 and a modern steel barge found in Israel, Denmark, Germany and Norway respectively. All seismic surveys were carried out slightly different from each other but employed the use of high frequency chirps (2KHz – 23KHz). In Israel, the seismic survey took a traditional approach with a profile perpendicular to the longitudinal axis of the shipwreck. This approach imaged the shipwreck as shown in figure 4.

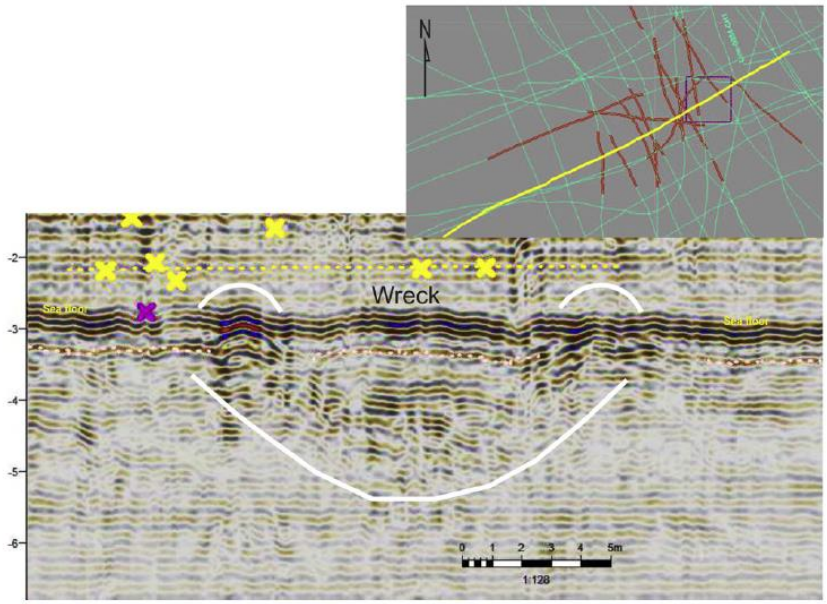

Figure 4 Akko 4 shipwreck embedded 1.5m in the sea floor (Grøn et al., 2015)

In Denmark, the same instrument was used but it was to test how much time and distance between sailing lines to locate a specific wreck. In Germany, an analogue predecessor of the instrument was used in a survey covering all of Haithabu Nor. Finally in Norway, a digital predecessor of the instrument used at Akko 4 and sailing lines were conducted in an E-W trend. From their findings, good results can be obtained using off-the-shelf sub-bottom profilers. All instruments used were different generations of the same instruments. Sub-bottom profilers have a much greater potential for revealing shipwrecks embedded in the sea floor than diver surveys. A study done in the Belgian coast at Ostend-Raversidje (Missiaen et al., 2018) mentioned how shallow water environments have the most dynamic elements: fierce wave action, strong currents, and large tidal range - figure 5 shows the effects on their seismic survey acquisition. Moreover, the nearshore and intertidal areas are often marked by the presence of shallow gas severely limiting acoustic penetration. Their main goals were to map paleochannels and identify small scale archaeological artifacts using high resolution marine sub-bottom profiling complemented by terrestrial electromagnetic induction measurements (EMI). 2D and 3D seismic acquisition data, EMI and cores were the main methods used for data collection. From their results, 2D seismic data allowed to identify complex pattern of paleochannels and the 3D revealed several artificial subsurface features. However, the local presence of gas in the sediments and relative wide profile spacing made it difficult to follow and map all of the channels.

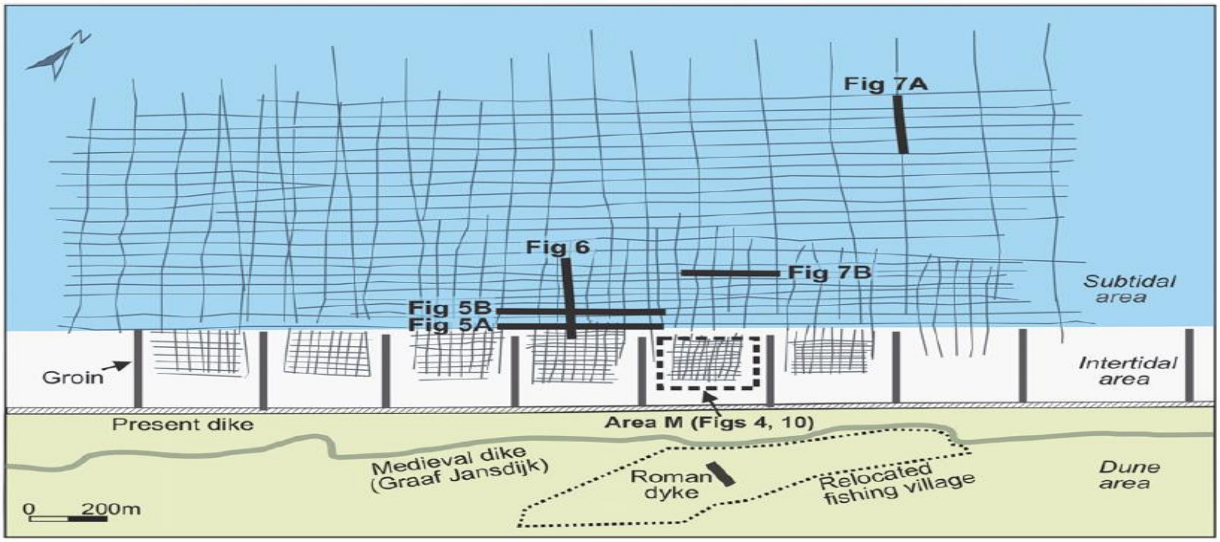

Figure 5 An irregular seismic grid due to dynamic elements (Missiaen et al., 2018)

A high resolution 3D seismic investigation of the Hedeby Harbour, Germany was conducted by Mueller et al., (2013). This work shows how automated seismic data processing can make acquisition results available on site few hours after the survey. The main goal, however, was to assess the extent to which marine 3D-seismic acquisition can help improve the complex but fragmented picture of Hedeby harbour. Equipment used for 3D seismic survey and acquisition was a SEAMAP-3D system consisting of an offshore acquisition component and onshore processing and imaging component. The results obtained lead to many open questions because of the confusing geological and potentially archaeological details. Additionally, free gas present in the sediments prevents penetration of the acoustic wave. Therefore, they concluded that 2D seismic reconnaissance should be done to identify areas of suitable penetration and 3D seismic acquisition. Object detection at shallow depths require ultra-high resolution seismic acquisition and processing methods. A SEAPMAP-3D seismic survey performed on marine archaeological sites near Iskele and Karantina Island in western Turkey to demonstrate that ultra-high resolution can be achieved in water depths of less than 2 m (Müller et al., 2009). The SEAMAP-3D system which consists of an offshore acquisition and onshore processing and imaging component, the seismic source was a boomer emitting acoustic frequencies between 100 Hz and 6000 Hz. 2D reconnaissance surveys were performed to evaluate seismic penetrability and pinpoint areas of interest for further investigation with the ultra-high resolution 3D survey. A submerged harbour structure was chosen for the 3D survey even though seismic penetrability wasn't favourable. The survey covered an area of 350m x 30m. A second survey of 120m x 40m area was done close to the

south eastern shore of the Karantina Island. The first survey yielded clear images of the submerged structure in the harbour as shown in figure 6.

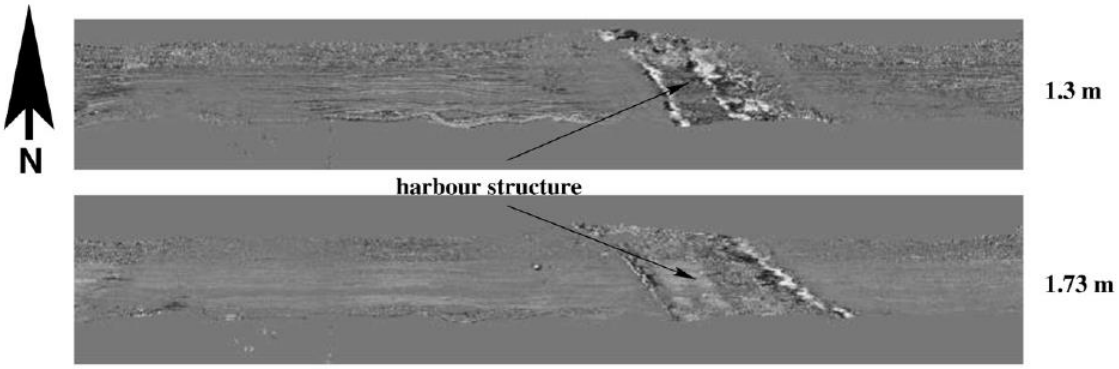

Figure 6 Time slice showing unmigrated 3D seismic data of the harbour (Müller et al., 2009)

For the second survey, due to hazardous boulders in the immediate shore vicinity and the survey being positioned 20m offshore. It couldn't be determined if there were any archaeological artifacts. Overall, the 3D seismic survey was of good quality, imaging the shore line, underlying sediment formation and local bedrock. Geophysical and geoarchaeological investigations in the Schleswig-Holstein, Germany were performed to map the remains and determine the state of perseveration of the medieval settlement of Rungholt and its southern dyke segment (Wilken et al., 2022). The study area came with its difficulties because it's located in a tidal flat environment making several geophysical techniques not feasible. First, saline water attenuates the ground penetrating radar and there is a narrow time window where the area is accessible during a low tide. Second, the investigation area lies about a kilometer from Hallig Südfall which has to be considered due to the narrow tide window. Data collection was done with magnetic gradiometry data, marine reflection seismic data, percussion core samples and aerial photography. Magnetic gradiometry survey was performed using six fluxgate gradiometers with an internal vertical sensor of 0.65 m, a horizontal sensor spacing of 0.5m and a sampling frequency of 20 Hz. A high resolution to channel seismic reflection system was used for the marine reflection seismic acquisition. The system creates a signal of 2 kHz to 6 kHz and a peak frequency of 3.5 kHz. Bandpass filtering, deconvolution, automatic picking of the seafloor reflection, semblance-based coherence filter, geometrical spreading correction and Stolt migration were performed on the seismic data. Finally, sediment cores were drilled at selected areas. From the results, magnetic gradiometry and coring during low tide and marine reflections during high tide are highly suitable for imaging and understanding the near surface areas of North Frisian,

Wadden Sea. As shown by several studies, shallow waters are sensitive to several factors especially source-receiver configuration. In Baradeloo & Carcione (2008), the source used for the acquisition was a boomer placed at a constant depth of 10 cm to reduce dragging turbulence. A multi-hydrophone streamer consisting of eight equidistant piezo-electric elements was used as a receiver system. Frequency band was 0.4 – 9 kHz with a notch frequency of nearly 7.5 kHz. Suitable floaters kept the streamer as shallow as possible to avoid destructive interference. Traditional seismic data acquisition is done having the streamer towed behind. In their study, they proposed and used a transverse geometry to collect more coherent events. The results (figure 7) showed that it is possible to perform high-resolution seismic surveys with a single-channel, multi-hydrophone streamer in shallow water using a transverse source-receiver configuration.

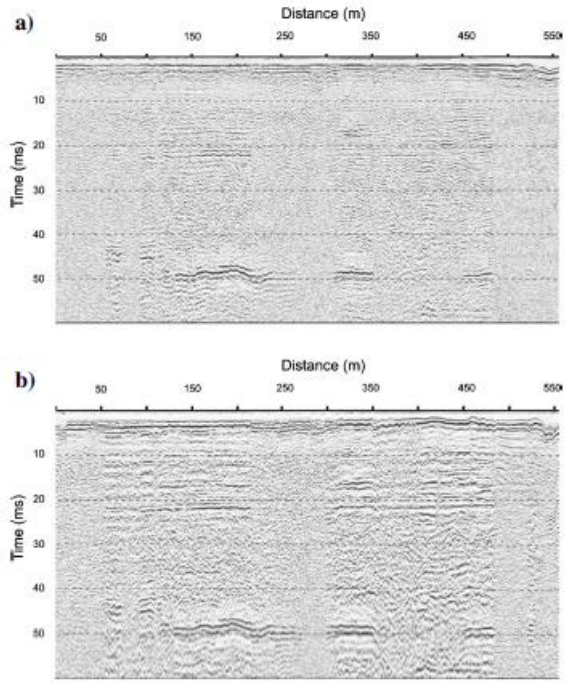

Figure 7 Conventional (longitudinal) geometry survey (a). Transverse geometry survey (b). Horizontal distance versus two-way traveltime is shown (Baradello & Carcione, 2008).

The signals recorded by the hydrophones are stacked to produce a more coherent signal than a longitudinal configuration. Different marine seismic reflection techniques have been progressively used over the years to investigate and locate submerged geomorphological and archaeological sites. High-frequency seismic profiling systems is used for sub-bottom imaging allowing a non-intrusive view of material below the seabed. Winton (2019) conducted research that quantifies the accuracy and variability associated with non-invasive parametric SBP measurements of shallow depths and the potential relationships between

acoustic wave parameters and types and condition of a variety of buried material. In situ experimental burial surveys were conducted, different timber types were buried in sediment environments representing the environment which maritime archaeological material lies buried. A comparative in Situ site – James Matthew ship - was investigated. A sub-bottom profiler - Innomar SES-2000 compact SBP – has a sampling ping rate of up to 40 pings/second and data acquisition rate of 70 kHz . From the seismic acquisition results, the quantification and accuracy with non-invasive parametric SBP measurements of shallow buried maritime archaeological material was proven by the in situ experimental survey. The interpretation of SBP measurements of the James Matthews wreck-site showed different reflection characteristics from known locations of slate, iron and timber. Submerged archaeological features and the position of the coast relative to the shoreline is dynamic (Jaijel et al., 2018). Sea level changes, sediment transport, erosion, deposition and a possible combination of those can change a coastal marine area into a modern terrestrial feature by infilling or subsiding the coast because of sea level rise. (Jaijel et al., 2018) focus on the ancient Maya coastal site of Vista Alegre, located in the north coast of Yucatan Peninsula, Mexico. Shallow seismic survey was performed in the waters surrounding Vista Alegre, using the SyQwest Stratabox specifically designed to work in shallow coastal environments. The system outputs a high frequency of 10 kHz; however, the operator has little control of the acoustic signal. From the seismic data acquisition results, two buried basins were revealed separated by a ridge and interpreted seismic horizons provided evidence of sea-level rise revealing an ancient shoreline. Therefore, sub-bottom profiling in shallow coastal areas are useful in choosing the best areas for future underwater archaeological excavation work. Marine archaeologists are interested in detecting artificial structures of sunken historical settlements in flooded areas due to increasing sea level (Wunderlich et al., 2005). Numerous problems have been identified during acoustic detection of embedded objects, the most known problem being small object dimensions (Müller & Wunderlich, 2003). To tackle these problems, a nonlinear acoustic approach was used in detecting and mapping embedded wooden objects (figure 8) dating from the Viking era in very shallow water. Two signals of slightly different high frequencies are simultaneously transmitted at high sound pressures. Results from the nonlinear seismic survey showed that small-sized embedded objects can be seen particularly well using oblique sound beams. This proved that the use of nonlinear sub-

bottom profilers offers many advantages over linear ones.

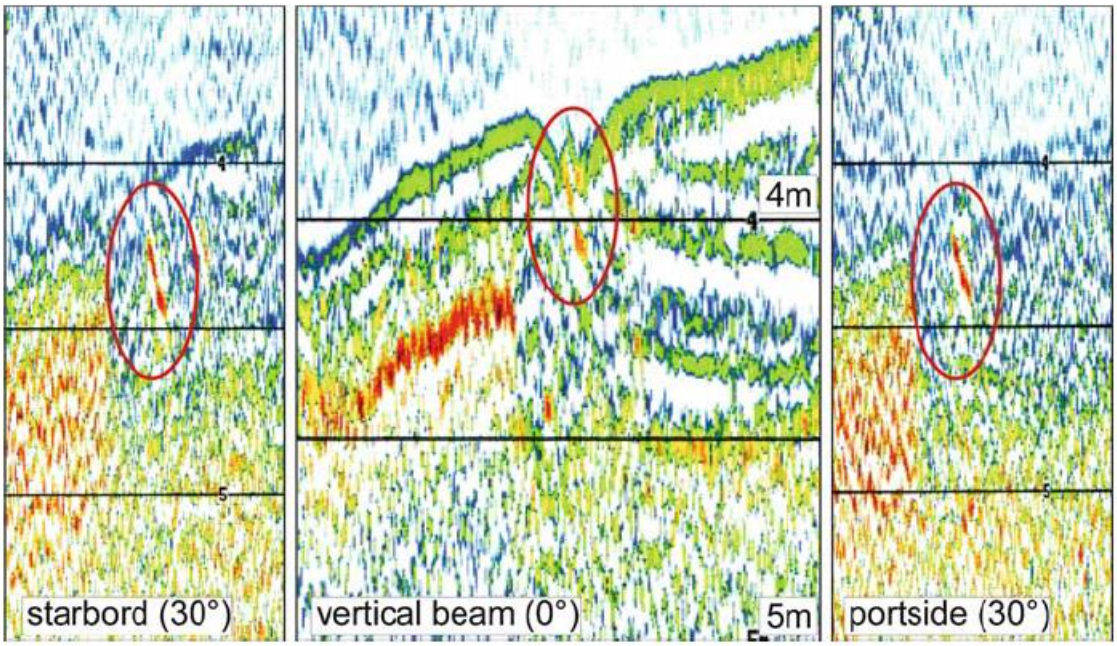

Figure 8 Echo plots of vertical and oblique beams of the same buried object at different profile lines (Wunderlich et al., 2005)

Therefore, archaeologist dealing with submerged small-sized objects will greatly benefit from nonlinear sub-bottom profilers due to small objects being detected particularly well by using oblique sound beams. 3D seismic cube can be acquired by setting the sailing lines of a conventional single-channel sub-bottom profiler to a dense configuration (Shin et al., 2022). This study was focused on the 3D seismic acquisition capabilities of the EOS wing – a 3D sub-bottom profiler. The CHIRP of the EOS wing study has a frequency range of 10 Hz – 20 kHz. One important step in 3D seismic processing is 3D binning where different sailing lines and different receiving channels on the same cell corresponding to the mid-point of the source and receiver are stacked into one representative trace. 3D seismic acquisition was performed offshore near Ulsan, South Korea. Data processing were done in two stages: stage 1 is performed internally in the general single channel CHIRP and stage 2 is in-depth data processing performed to produce a 3D seismic cube (first-arrival picking, tidal correction, normal move-out correction and 3D binning). The 3D seismic cube showed the irregular seafloor which clearly appears in the cube. Steep slopes, thin reflectors parallel to the sea bottom and acoustic blanking zones were observed. The acoustic blanking zones was due to the acoustic signal not able to transmit because of the presence of gas. In conclusion, the EOS Wing system was able to image various geological features, including irregular seafloor,

parallel strong reflection, acoustic blanking zones and channel-fill structures. This proves that 3D CHIRP can be efficiently used for practical geological research.

Study Area and Data

The first study area is located close to St. Olaf's church in Avaldsnes (figure 9). Avaldsnes is a village in the northeastern part of the Karmøy municipality in Rogaland, Norway. The 3D seismic survey was done in the waters located at the southeastern part of the Avaldsnes church. The church has been an important place not only for archaeology but also historically. The church was built around 1250 by King Håkon Håkonsson in Avaldsnes, Norway. After 1536, the church fell into ruin and restoration was conducted and finished in 1929. Several small archaeological investigations and excavations have been going on for the last 20 years. This has led to several discoveries of iron age, medieval times (Vea, 2017). A restored Viking farm is located fifteen minutes away by foot from St.Olaf's Church, Avaldsnes. There a longhouse, boathouse for a Viking warship, a roundhouse, and several small buildings can be found.

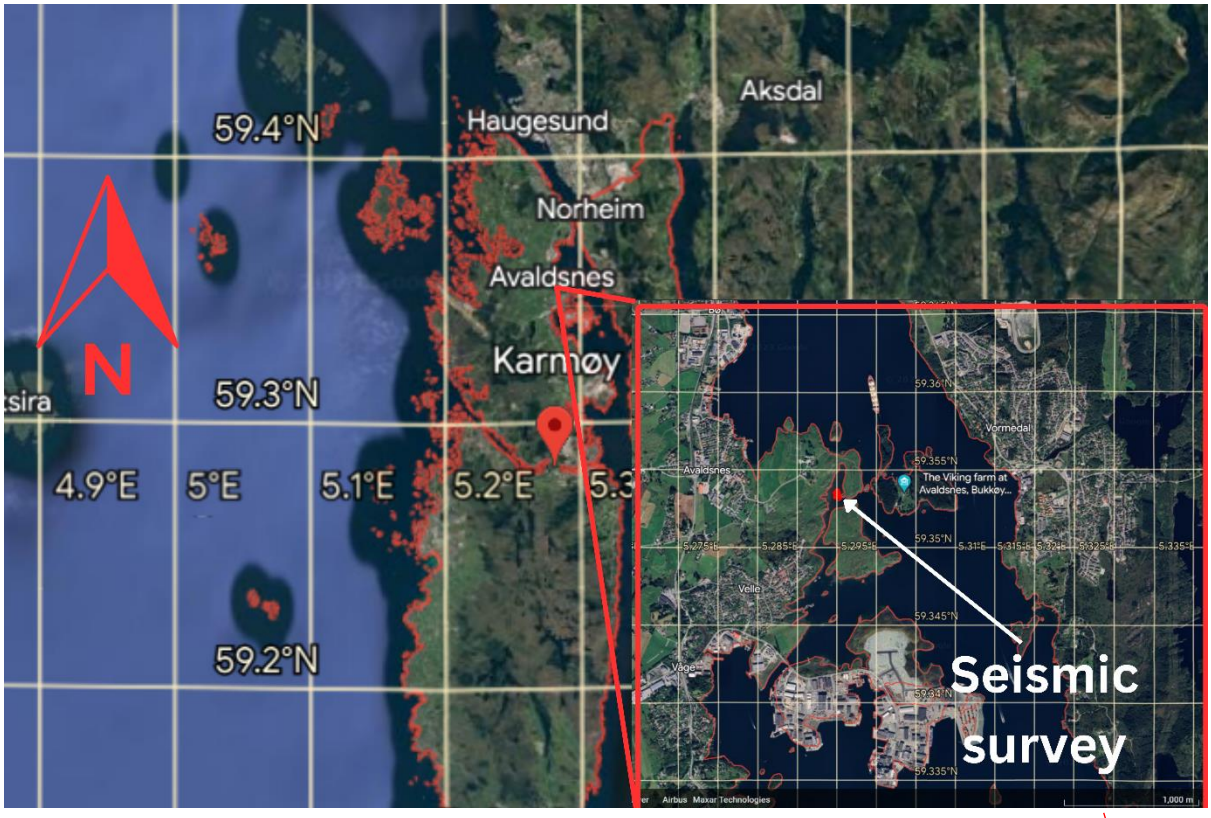

Figure 9 Location of Avaldsnes and seismic survey

The second study area is located in, Hafrsfjord (figure 10). Hafrsfjord is a fjord in the Sola and Stavanger municipality in Rogaland, Norway. The fjord is of the most historically and

archaeologically important places in Norway. Hafrsjord is where, according to the Sagas, - King Harald, the first king of Norway won a great naval battle during the year 872 resulting in the unification of Norway. Despite the stories, no archaeological evidence exists to support this historical claim. Nonetheless, in the waters of Hafrsfjord lies the remains of a Sailboat from the 18th century, which is one the targets of this thesis.

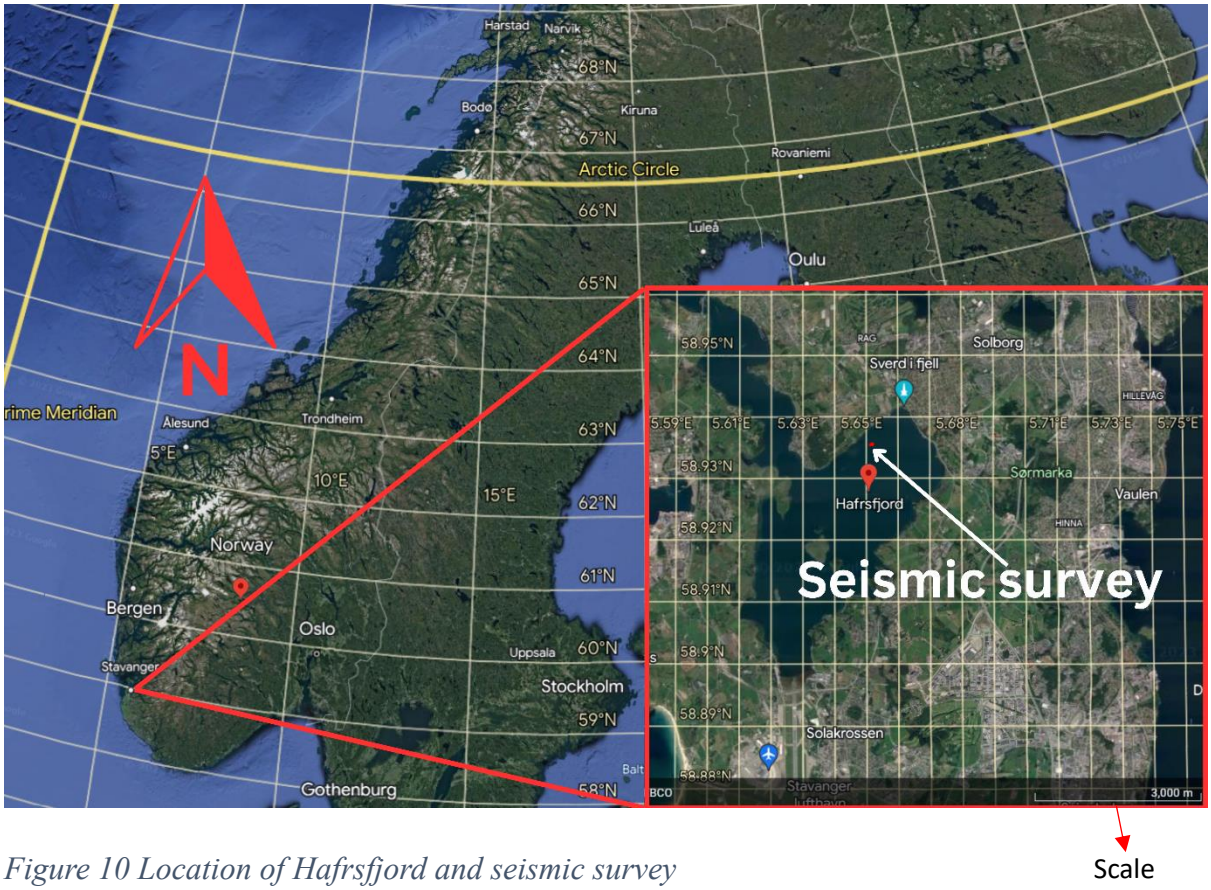

Figure 10 Location of Hafrsfjord and seismic survey

Data and Methods

Buried archaeological materials can be detected with marine geophysical techniques that use acoustics due to the contrast between the material and the surrounding water column or sediments (Bull et al., 1998). This allows the imaging of buried archaeological materials by calculating the reflection coefficients (Arnott et al., 2005). Laboratory measurements of the compressional wave velocity, bulk density of oak and pine samples, for varying states of decay, were done (Winton, 2019). From the data, theoretical reflection coefficients for such materials can be calculated. The theory was tested against two wreck sites: Invincible wreck site at Horsetail Sand, East Solent, UK and a wreck in St. Peter Port Harbour, Guernsey. The results of this study show that, - reflection coefficients decrease with increasing degradation. The magnitude of the reflection coefficients varies with both sediment type and wood species. Additionally, the longer a wooden archaeological artifact has been submerged the

more difficult it becomes for geophysical methods to identify it. The wreck site in Guernsey is an example of the wreck not being imaged due to the similarity of the reflection coefficients of the water and the timber. For the Invincible site, a seismic image was possible, however, reflection coefficients show the oak timbers were heavily degraded. By considering the reflection coefficients, one can tell the state of degradation improving the wreck assessment and detection.

Seismic Equipment and Data Collection

The data used in this study was collected using a single-channel high-frequency sub-bottom profiler (Chirp) produced by MERIDATA (figure 11). The source signature consists of a non-linear sweep (Chirp) with a frequency range between 10 and 20 kHz. The Chirp source was mounted on an autonomous acquisition vessel (Olsen et al., 2023). The single channel transducer acts as a source and receiver making the seismic acquisition a zero-offset acquisition. One important characteristic of this system is that the emitted seismic wave is dip limited, which means that the transducer sends and receives over a cone with an opening angle of 40 degrees.

Figure 11 MERIDATA Sub-bottom profiler with a submerged chirp

The chirp is fully submerged in water sending acoustic energy which is dependent on the configuration. In this study for every 0.25 seconds, the chirp sends out an acoustic signal and records the reflected wave for time length of 100 ms. With an average speed of 0.7 m/s, this represents a trace acquired every 17.5 cm in the sail direction. The nominal vertical resolution of the system using a half-wavelength criterion in average water velocity conditions and with a dominant frequency of 15 kHz is 5 cm. Estimation of the horizontal resolution is more difficult, because of influence of the water depth and the directivity of the source. A real-time-kinematic DGPS is used to obtain the coordinates of each of the traces in the survey. In principle, x and y coordinates as well as elevation can be obtained from GPS measurements. However, in the seismic surveys used in this work elevation was not logged. The seismic processing unit records the raw signal performed as basic seismic processing (deconvolution and a positive signal envelope) on the recorded data and saves the data as a SEGY file.

Seismic Data Acquisition

Avaldsnes

The 3D fullwave dataset has 51705 traces and, 1501 samples per trace with a sampling interval of $1e^{-5}$ seconds respectively. The distance between each survey line is approximately 0.25 m (figure 12). The area of the seismic survey was approximately 1,519 m^2. The water depth at the start of the seismic survey acquisition was found to be 0.58 m. Due to the time constraints associated with the dropping tide, only inlines were acquired.

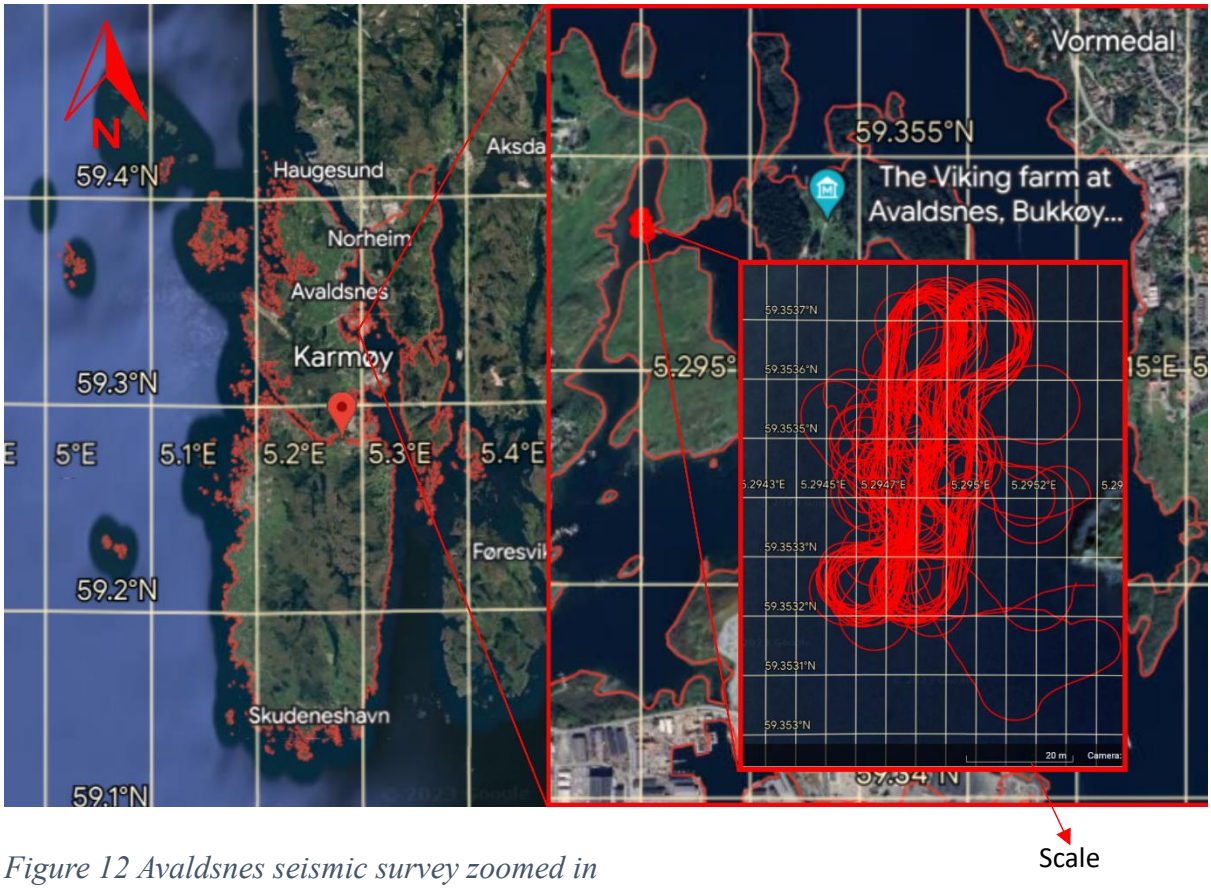

Figure 12 Avaldsnes seismic survey zoomed in

Hafrsfjord

The seismic acquisition was done in the waters of Hafrsfjord (figure 13). Fullwave and envelope data were recorded in the survey. The envelope data has 33901 traces, 5501 samples per trace with a sample interval of $4e^{-5}$ seconds, and the full wave has a total of 36648 traces, with 22001 samples per trace with a sample interval of $1e^{-5}$ seconds. The distance between each survey line is approximately 0.25 m. The area of the seismic survey was approximately 1000 m^2 (inlines and crosslines) and the water depth was approximately 40 m.

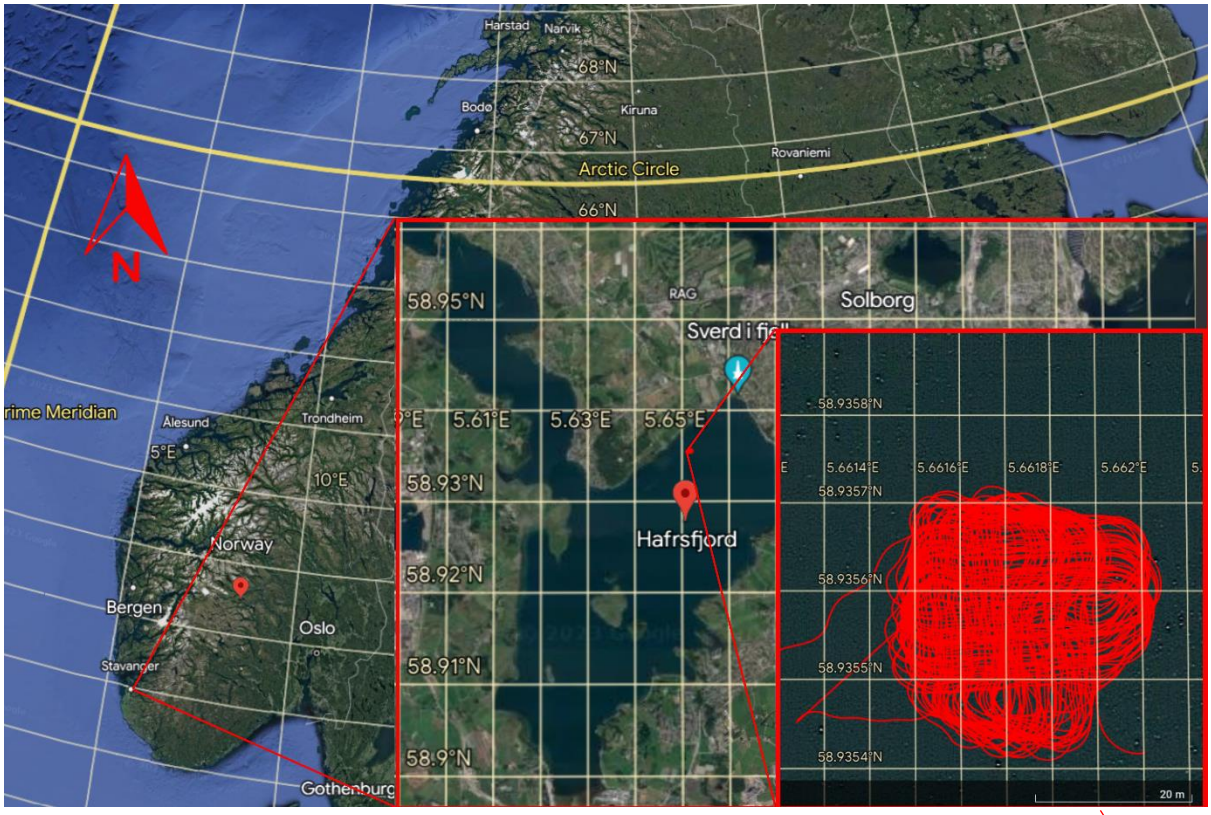

Figure 13 Hafrsfjord seismic survey zoomed in

Seismic Reflection Theory

The subbottom profiler used in this work exploits the principles of marine seismic reflection. The geophysical method of marine seismic reflection consists in sending artificially generated acoustic waves that propagate through the water and into the seafloor. Different structures and objects within the Earth's crust may reflect some of these waves and it is these reflections that are recorded by receivers (hydrophones or geophones) and used to image the subsurface. The reflection strength of the waves depends on the contrasts in the acoustic impedance (a product of the density and seismic wave speed) across the different reflectors in the subsurface. These recorded waves are processed to produce a visual representation of the sub-surface (Micallef, 2011). Shot gather, common receiver gather, common midpoint gather, common offset gather and zero offset gather are a few ways to conduct a seismic survey. Zero offsets gather or acquisition is when there is no horizontal distance between the source and receiver (figure 14), which is the configuration of the sub-bottom profiling system used in this thesis work.

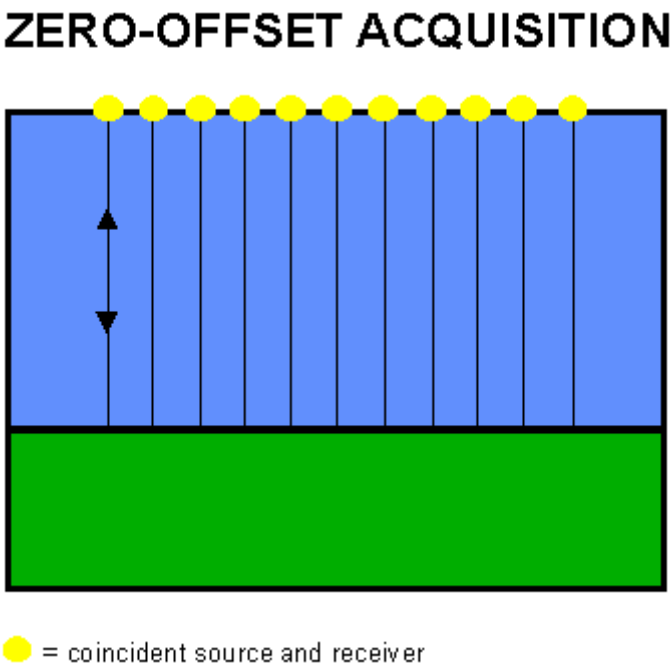

Figure 14 Zero offset acquisition (source and receiver marked as yellow) (XSGeo, 1999)

Furthermore, the sub bottom profiler's chirp is a source and receiver (figure 15) and therefore makes the seismic acquisition zero offset. The formula for zero offset acquisition is represented by:

$$T(x) = \frac{2D}{V}$$

Where T(x) is the time taken for the wave to travel, D is the distance and V is the velocity of the wave. Seismic resolution is defined as the smallest distance between two objects such that they can still be individually distinguished in a seismic image. Seismic resolution can vary significantly on the direction and is often considered split into horizontal and vertical resolution. Vertical resolution is the smallest thickness a geological can have before reflections from the top and bottom can no longer be distinguished from each other. While the horizontal resolution is the smallest distance that enables distinguishing between two laterally displaced features in a seismic image. Seismic resolution is controlled by the bandwidth of the signal (Chopra et al., 2006). Vertical resolution can be estimated using the formula below:

$$\delta z = \frac{1.5\lambda}{4}$$

Where δz is the vertical resolution and λ is the dominant wavelength. Applying this formula to our chirp. We can compute the vertical resolution of the sub-bottom profiler. The operating

frequency of the chirp is 10 – 20 kHz. Computing the wavelength ($\lambda = V/f$, V = velocity in the water column, and f = frequency), we get a range of 0.075 – 0.15 m. That is assuming a velocity of 1500 ms^{-1} in the water column. Plugging these values into the vertical resolution formula, we get a range of 0.028 – 0.05625 m as the vertical resolution. This vertical resolution is in line with the vertical resolution stated earlier.

Figure 15 A close up image of the sub bottom profiler chirp

Seismic Processing

Tidal Correction

In Avaldsnes, the tides reach as high as 100 cm and as low as 12 cm (figure 16). This is the difference between the height of the tides. In Hafrsfjord, tides reach as high as 60 cm and low as 20 cm (figure 17). Due to the rise and fall in the water column throughout the day. The seabed is not representative in the seismic imaging. The rise of the water level causes the seabed to be at a deeper level and vice versa. Hence tidal correction is required to know the true depth of the seabed and reflections. To do this, the seabed reflection time was picked at positions surveyed redundantly at different times, such as the crossing of survey lines (figure

18a). The seabed reflections two-way time were plotted as a function of time of the day and a tidal function was derived for the tidal correction (figure 18f).

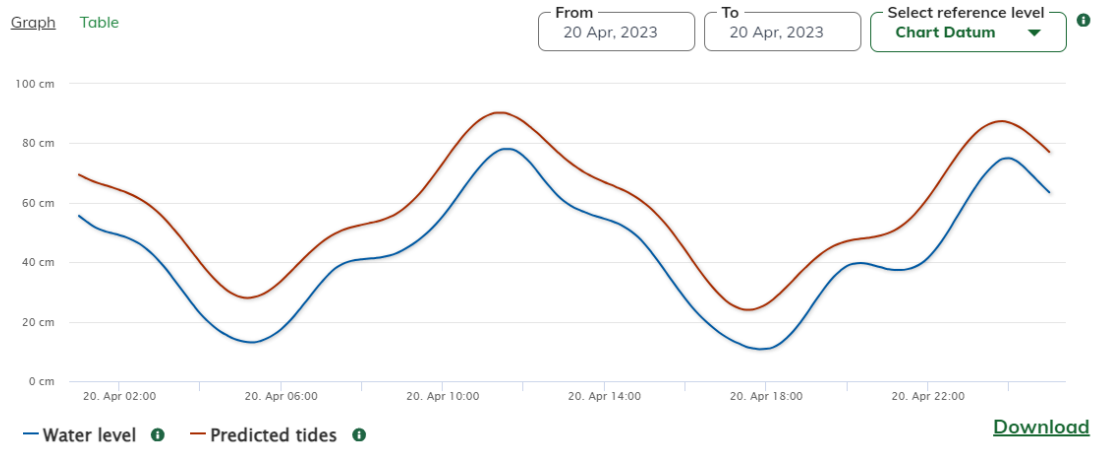

Figure 16 Tide variatian in Avaldsnes on the day of seismic acqusition (Kartverket, 2023)

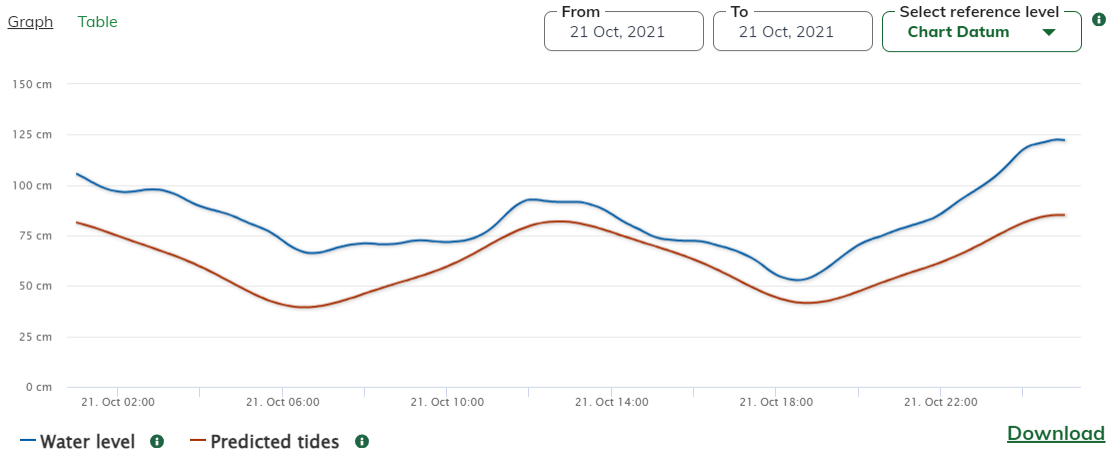

Figure 17 Tide variation in Hafrsfjord on the day of seismic acquisition (Kartverket, 2023)

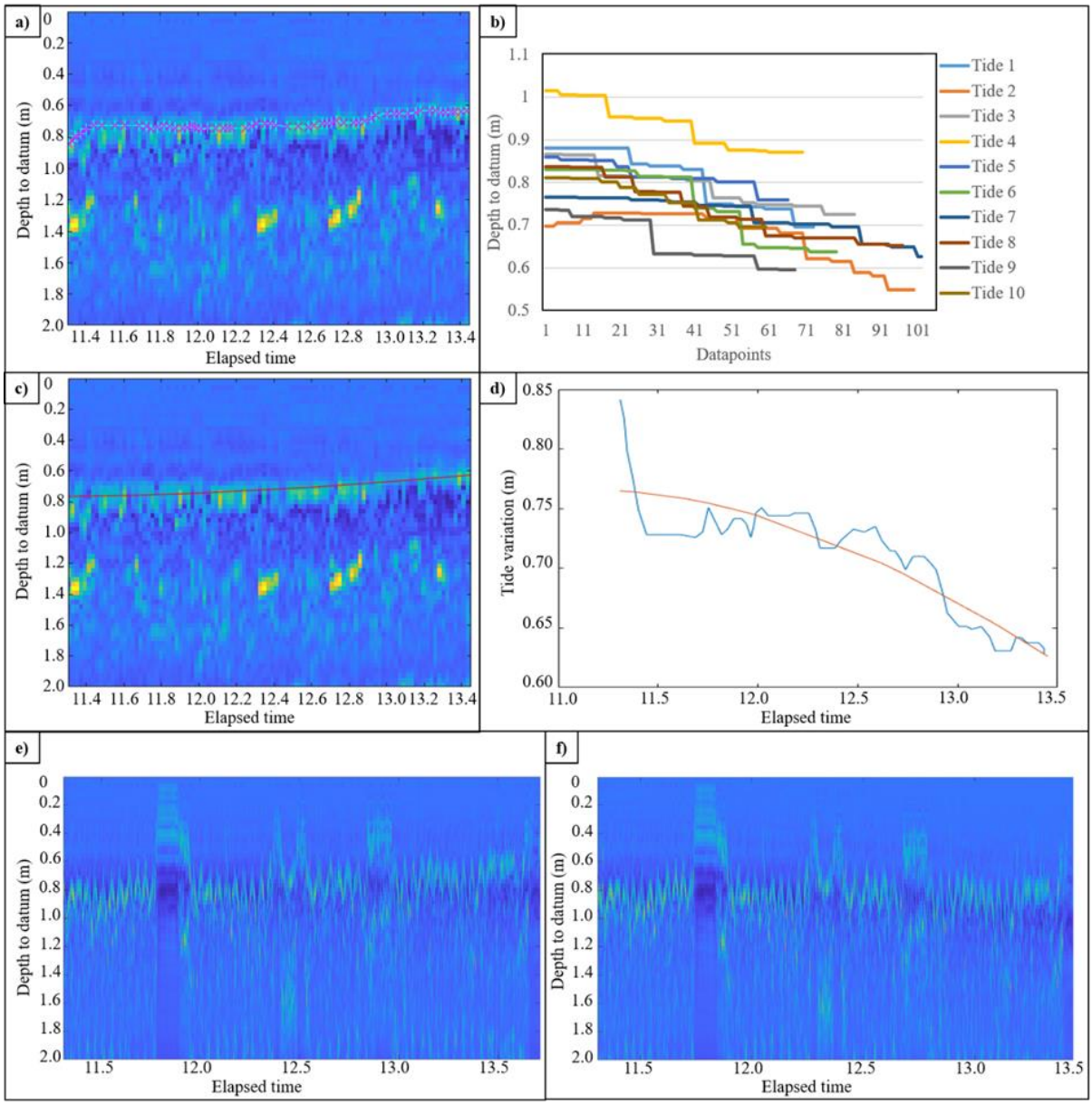

Figure 18 a) Manually picked sea floor; b) ten different locations are tested where the tide 7 location is most promising; c) picked sea floor in tide location 7; d) depth variation from 0.76 to 0.626 m; e) before tide correction and; f) after tide correction (Olsen et al., 2023).

Make 3D Grid

To interpolate the data points into a 3D cube, a regular grid had to be made for the seismic survey. It is on this grid that seismic data points will be interpolated. To create the grid, an in-house Python script was used. From this script, four corners of the regular seismic rectangle can be chosen to cover the seismic survey, and different spacings between inlines and crosslines can be set. In this thesis, grid spacings of 0.1 m by 0.1 m, 0.3 m by 0.3 m, and, 0.5 m by 0.5 m were tested (figure 19 and 20).

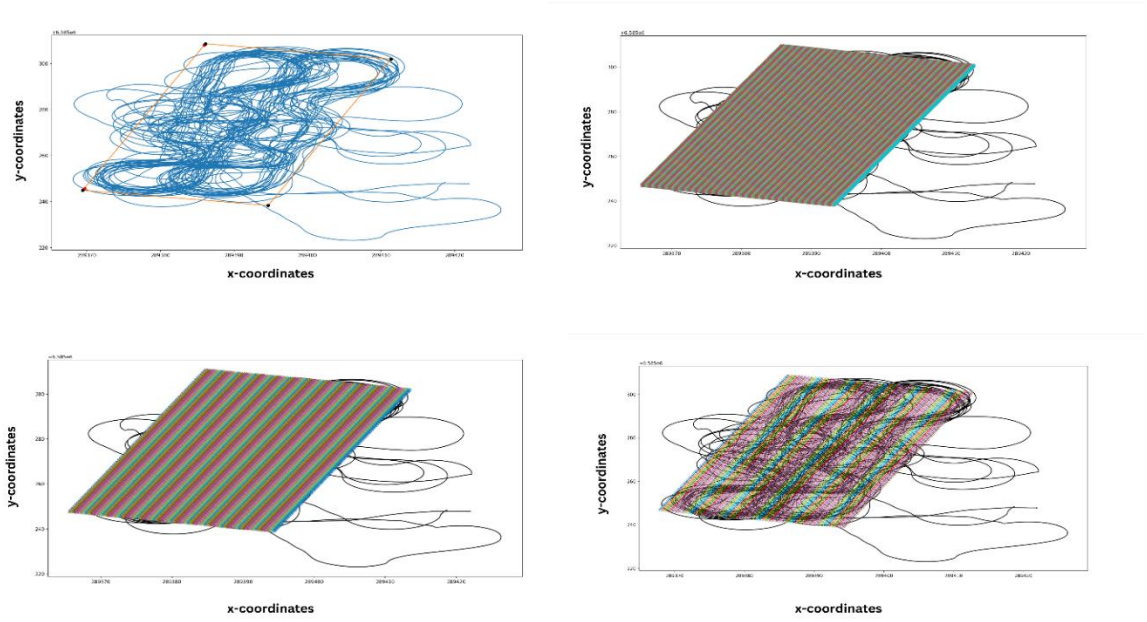

Figure 19 Making the 3D grid (top left) in Avaldsnes, 0.1 m by 0.1 m (top right), 0.25 m by 0.25 m (bottom left), and 0.5 m by 0.5 m (bottom right) grid sizes

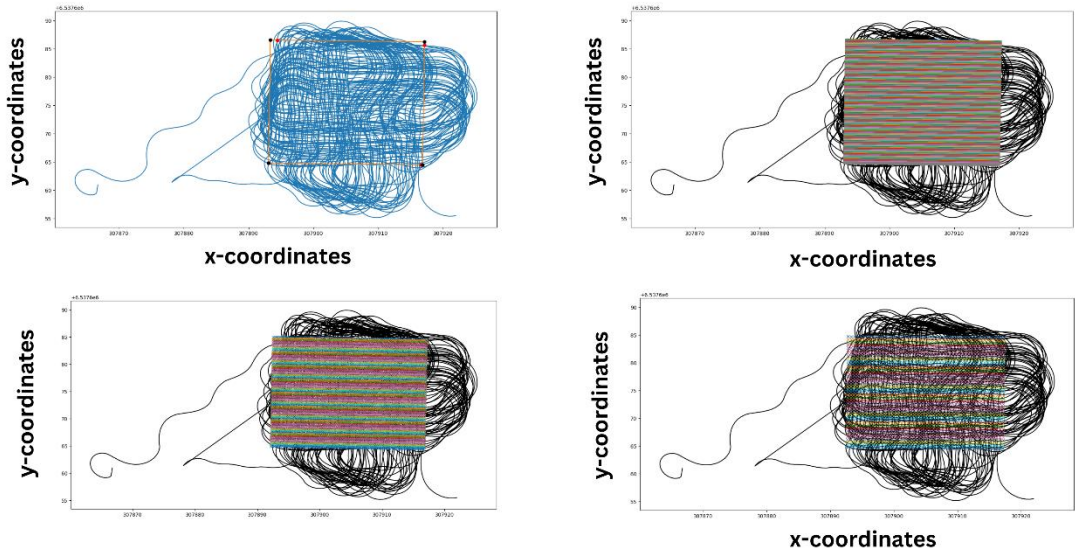

Figure 20 Making the 3D grid (top left) in Hafrsfjord, 0.1 m by 0.1 m (top right), 0.25 m by 0.25 m (bottom left), and 0.5 m by 0.5 m (bottom right) grid sizes

Binning

Once a regular grid has been created the next step was to bin the data. Binning – a data pre-processing technique – was done to group the seismic data and coordinate values into "bins" (figure 21). The bin sizes can be set with the recommended value being less than 0.5. Values higher than 0.5 will run the risk of having fewer data points to work with. Furthermore,

binning can be done by grouping the data points according to their mean or median. Both methods were tested and median binning provided better results than the mean – images were sharper.

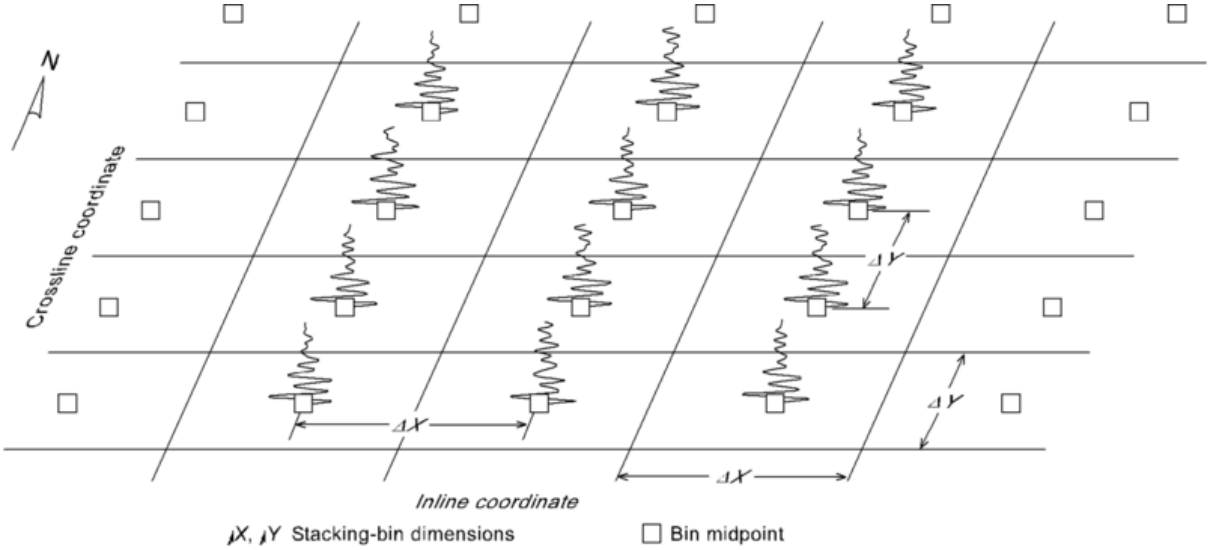

Figure 21 Seismic median binning processing (Producers, 2020)

Interpolation

Two interpolation methods were tested – Cubic and Shepard. Cubic interpolation constructs new points within the boundaries of a set of known points using multiple cubic piecewise polynomials (figure 22).

$$f(p_0,p_1,p_2,p_3,x) = (-\tfrac{1}{2}p_0+\tfrac{3}{2}p_1-\tfrac{3}{2}p_2+\tfrac{1}{2}p_3)x^3+(p_0-\tfrac{5}{2}p_1+2p_2-\tfrac{1}{2}p_3)x^2+(-\tfrac{1}{2}p_0+\tfrac{1}{2}p_2)x+p_1$$

Figure 22 Cubic interpolation formula

Shepard's interpolation, on the other hand, calculates the interpolated value which is the mean of values, weighted by inverse distance (figure 23). Using each of the interpolation methods on the binned data.

$$F(x,y) = \sum_{i=1}^{n} w_i f_i$$

Figure 23 Shepard's interpolation general formula

n – Number of points used for interpolation

f_i – Dataset values

w_i – Weight functions assigned to each points

The formula below shows how the weight function is calculated (figure 24):

$$w_i = \frac{\left[\frac{R-h_i}{Rh_i}\right]^2}{\sum_{j=1}^{n}\left[\frac{R-h_i}{Rh_i}\right]^2}$$

Figure 24 Shepard's interpolation weight function formula

n – Total number of points

R - Distance from the interpolation location to the most distant point

h_i - Distance from the interpolation location to the point *i*

Migration

The next seismic processing step was migrating the interpolated seismic data. Constant velocity migration from flat topography is more efficiently performed using Stolt migration. Furthermore, Stolt migration was preferred because of the lack of computational resources needed for kirchoff migration. The equation for Stolt migration is shown below (figure 25):

$$P(k_y, k_h, k_z, t=0) = \left[\frac{v}{2}\frac{k_z^2 - k_y^2 k_h^2}{\sqrt{(k_z^2+k_y^2)(k_z^2+k_y^2)}}\right] \times P\left[k_y, k_h, 0, \frac{v}{2k_z}\sqrt{(k_z^2+k_y^2)(k_z^2+k_h^2)}\right]$$

Figure 25 Stolt migration equation

y – midpoint

h – offset

t – event time in the unmigrated position

k_y, k_h and k_z – Fourier transfom variables

Migration was done using Stolt with a constant velocity of 1500 m/s - this velocity was chosen because it is the average velocity of sound in water (Aki & Richards, 2002). Apertures of 20° and 40° were tested to find the best results.

Results and Discussion

Interpolation

Cubic Interpolation

Avaldsnes

Figures 26, 27 and 28 show the interpolation results on the grid sizes – 0.1 by 0.1 m, 0.25 by 0.25 m and 0.5 by 0.5 m. Comparing all three grid sizes, the 0.1 by 0.1 m grid size shows the highest image resolution. Reflections are more consistent and do not have large amplitude

variations towards the higher numbers of the inlines and crosslines in the plot. This makes seismic interpretation easier because reflections are easily identifiable due to the fact that binning the grid size into small bins has a less smoothing effect although each bin will have less data points in the grid less bias. Whiles on the other hand, the larger bin size has more data points causing a large bias affecting the interpolation and creating a smoothing effect. Furthermore, the 0.1 by 0.1 m grid has the sharpest resolution and identifying the shipwreck is a bit of a challenge. This decreases with increasing grid size with the 0.5 by 0.5 m grid size having the lowest image resolution but shipwreck being easily visualized. The shipwreck makes a synclinal bowl shape in the inline and crossline of all three seismic images generated by each of the grid and the time slice shows the outline of the shipwreck.

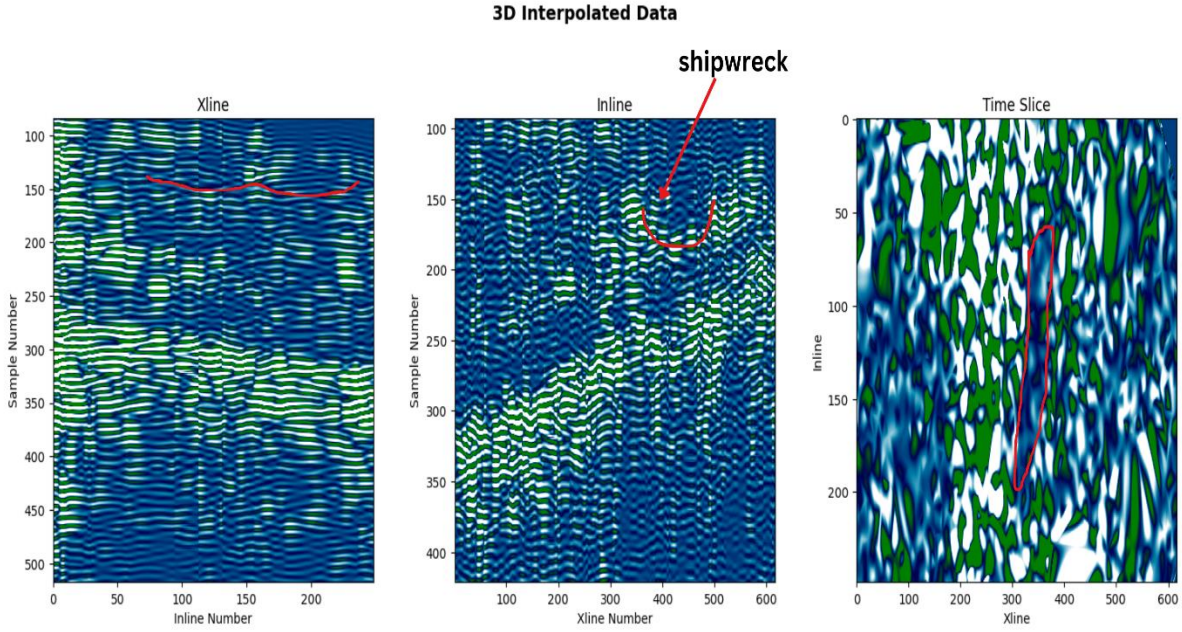

Figure 26 0.1 by 0.1 m grid size cubic interpolation result in Avaldsnes

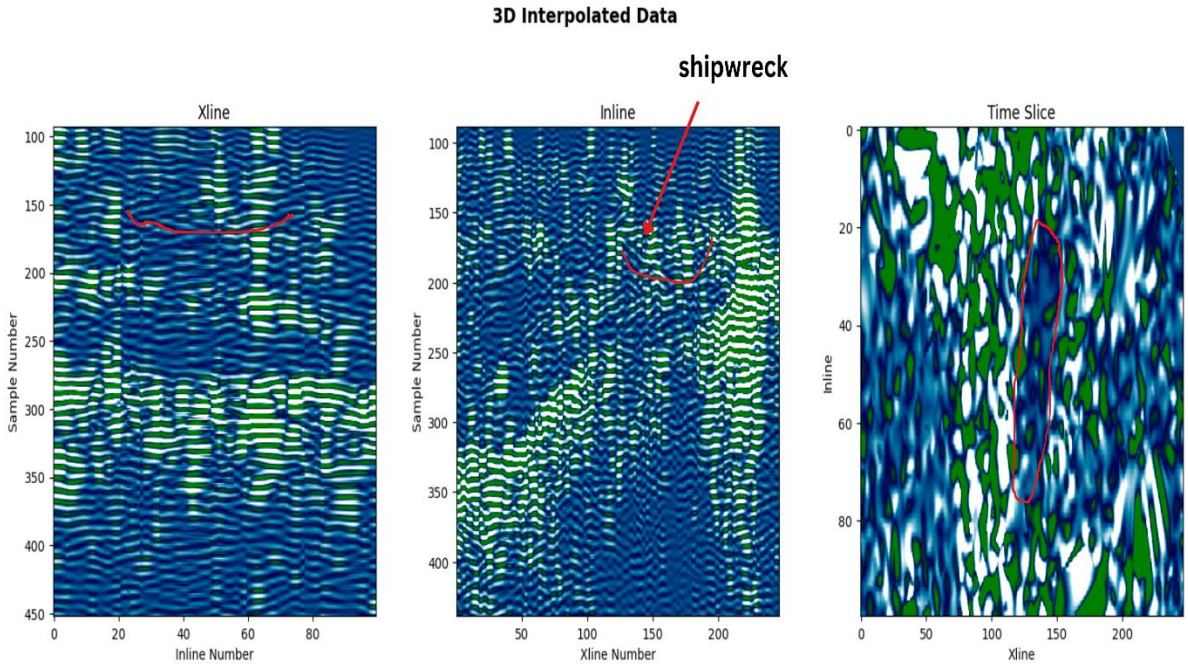

Figure 27 0.25 by 0.25 m grid size cubic interpolation result in Avaldsnes

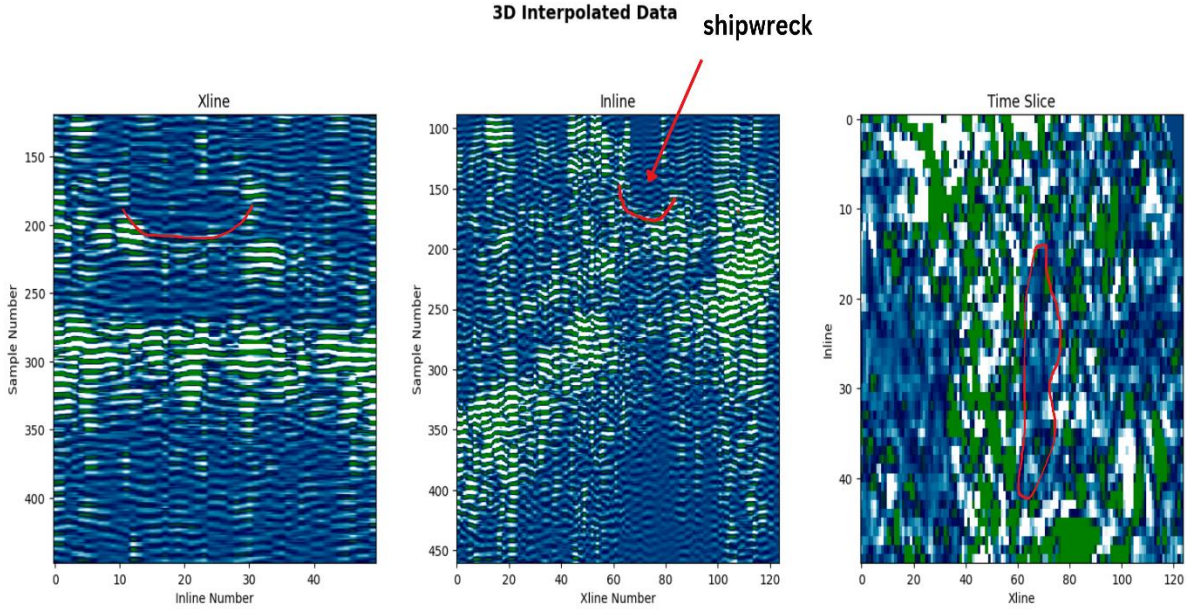

Figure 28 0.5 by 0.5 m grid size cubic interpolation result in Avaldsnes

Hafrsfjord

Envelope

In figures 29, 30 and 31, the interpolation seismic data shows the shipwreck to be lying on the sloping seabed. The shipwreck appears as a massive bump due to the wave diffractions on the seabed whereas in Avaldsnes, the shipwreck shows a bowl shape outline (figures 26, 27 and 28). In the time slice, bump causes a distortion or blurriness in the image compared to its surrounding areas. Comparing the seismic image resolution, the 0.1 by 0.1 m grid size has the highest out of the three, followed by 0.25 by 0.25 m grid size and 0.5 by 0.5 m grid size having the lowest resolution with the seismic images being pixelated. Although identifying the shipwreck was not a difficult task. The reflections in the image become smooth almost to the point of appearing as a single reflection. This smoothness decreases with decreasing grid size. Any bigger grid size will have caused the reflections to merge into one. Therefore, as mentioned earlier, bigger bins and grid sizes create a smoothing effect making it difficult for seismic interpretation.

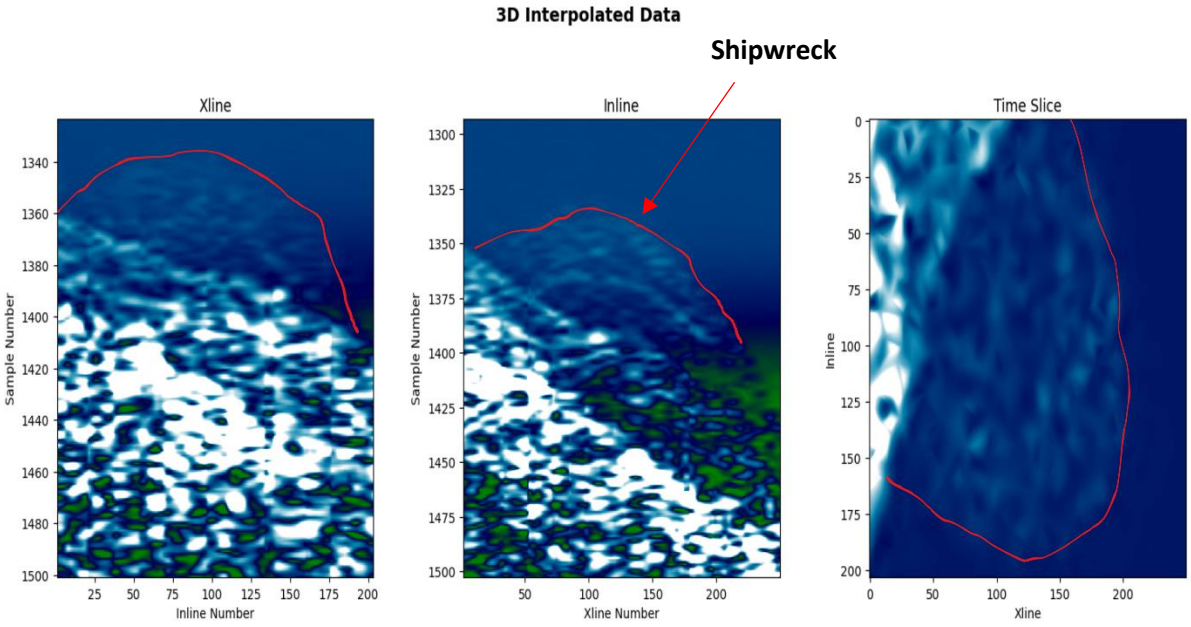

Figure 29 0.1 by 0.1 m grid size cubic interpolation result in Hafrsfjord

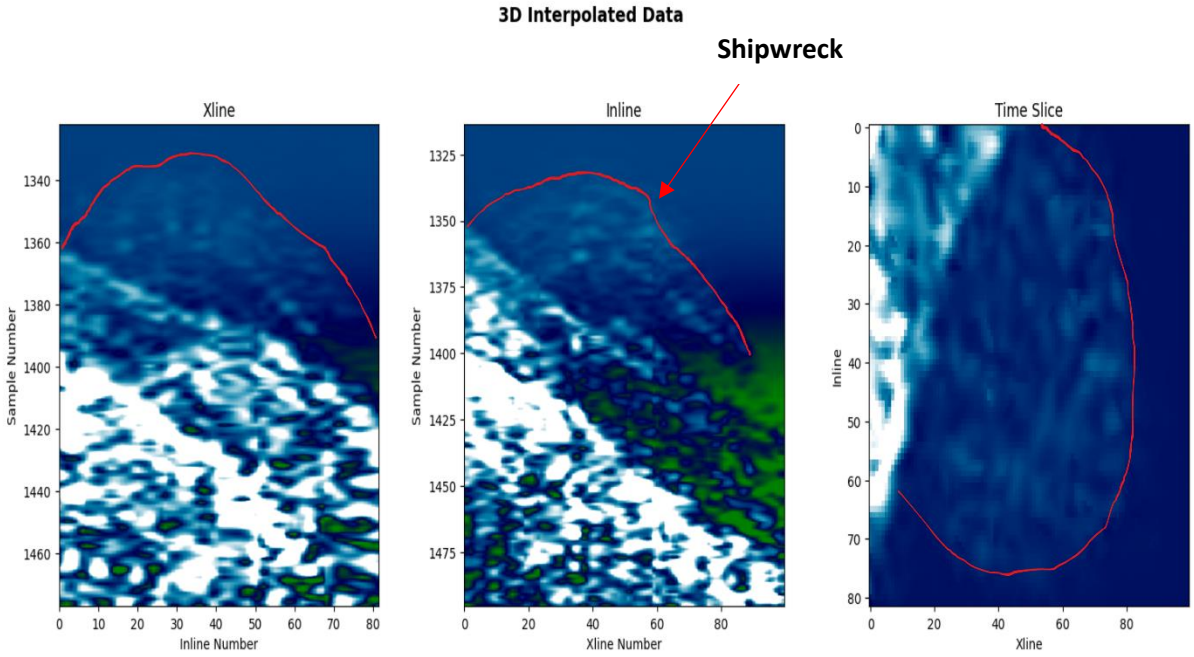

Figure 30 0.25 by 0.25 m grid size cubic interpolation result in Hafrsfjord

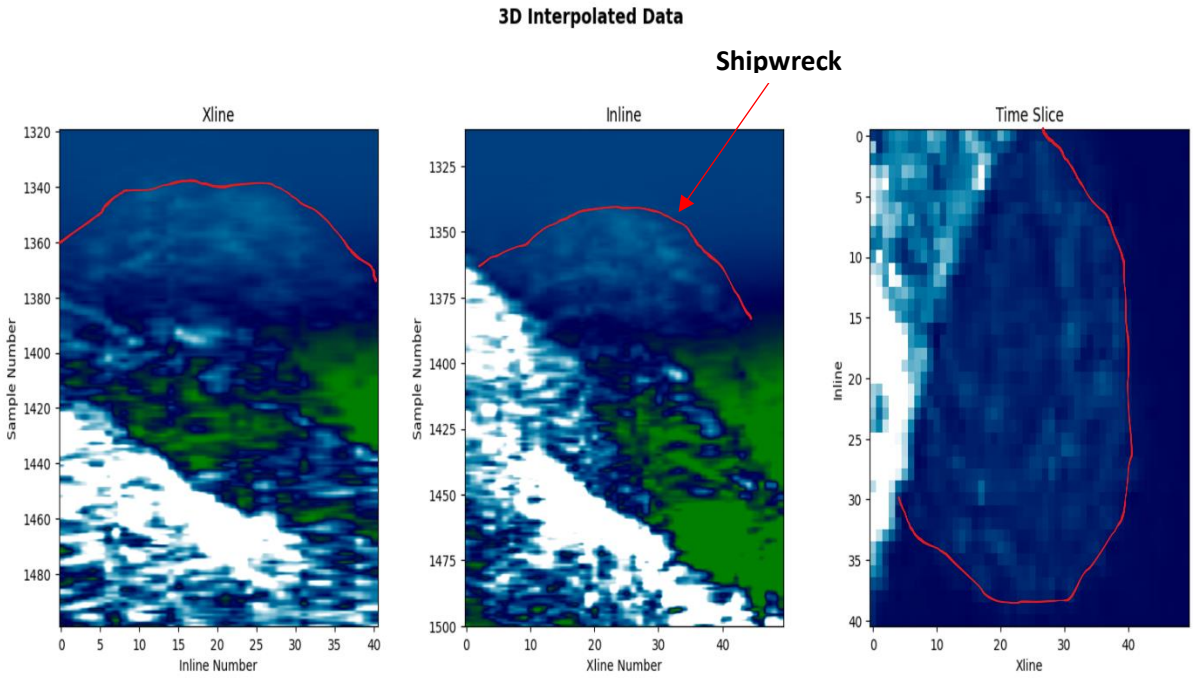

Figure 31 0.5 by 0.5 m grid size cubic interpolation result in Hafrsfjord

Fullwave

Figures 32, 33 and 34 show the cubic interpolated results of Hafrsfjord. Identifying the shipwreck was a challenge. The length of the boat in addition to the discontinuity of the reflections made it difficult to know the extent of the boat. The shipwreck appears as a synclinal shape compared to the “bump” in the envelope data (figures 28 to 31). In the time slice, the shipwreck was impossible to identify. There was no outline that matched the shape of the shipwreck. Overall, the 0.1 by 0.1 m grid size has the highest image resolution, however, identifying the shipwreck in the time slice was not possible. Although this is the case for every grid size, it is easiest to identify the shipwreck in 0.5 by 0.5 m grid size – inlines and crosslines (figure 34).

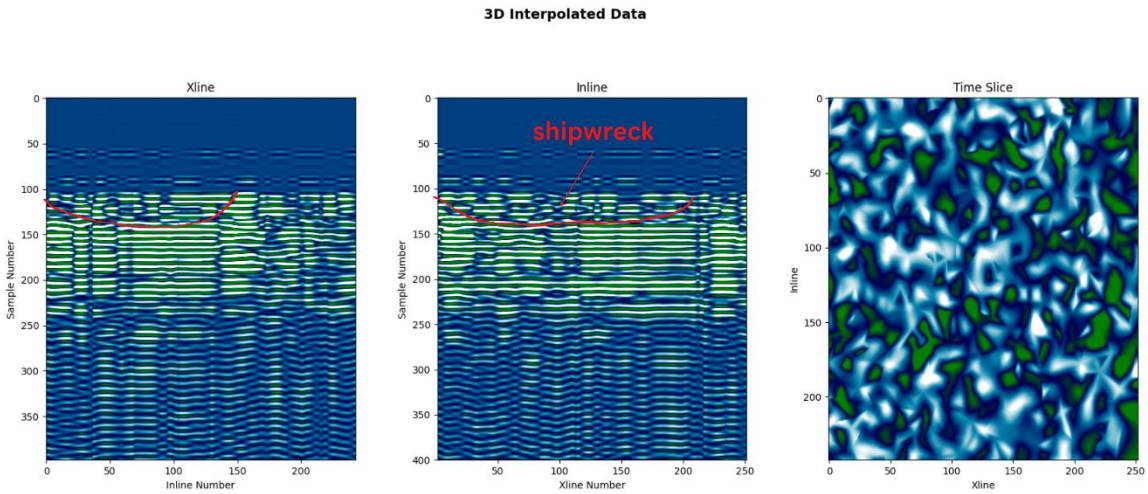

Figure 32 0.1 by 0.1 m grid size cubic interpolation result in Hafrsfjord (fullwave)

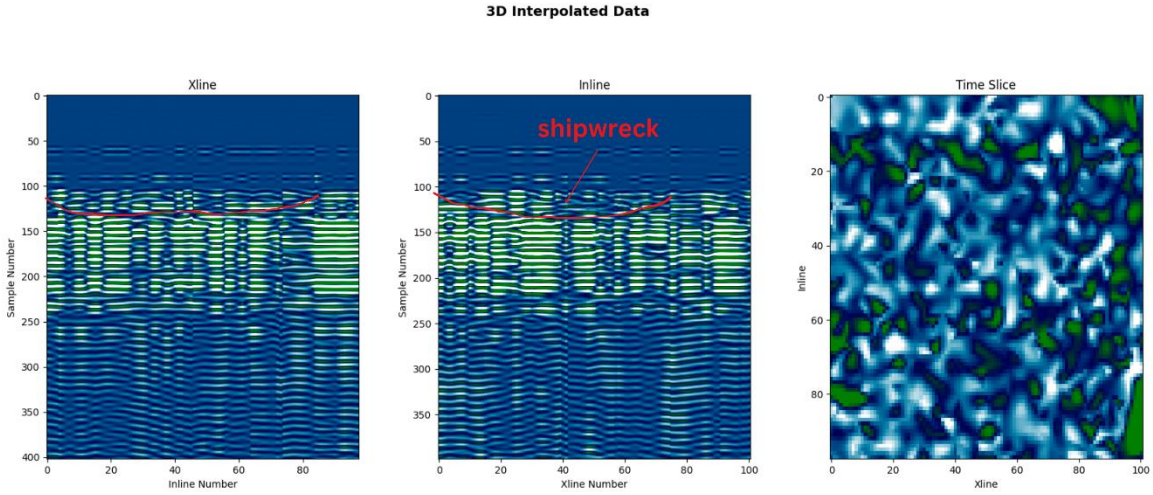

Figure 33 0.25 by 0.25 m grid size cubic interpolation result in Hafrsfjord (fullwave)

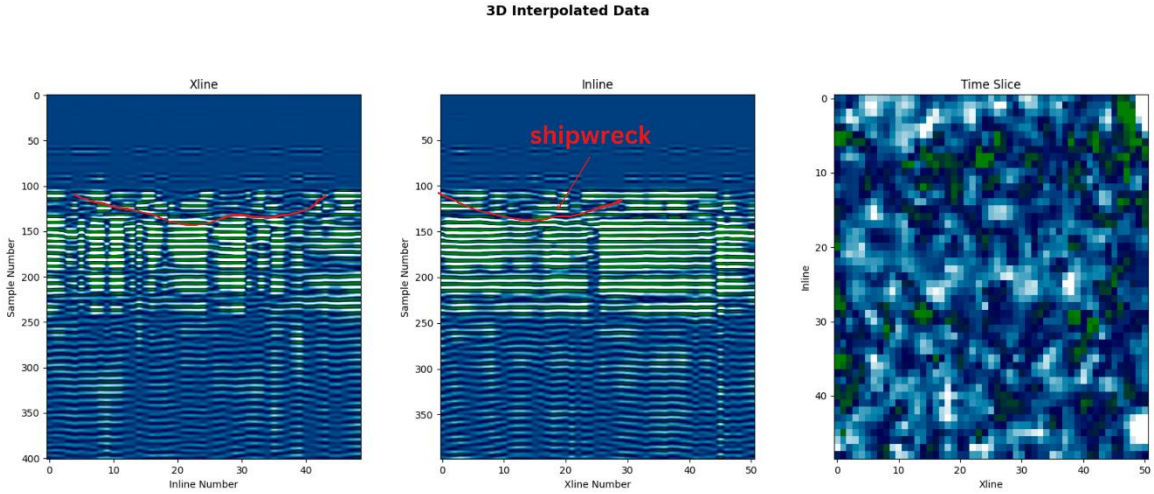

Figure 34 0.5 by 0.5 m grid size cubic interpolation result in Hafrsfjord (fullwave)

Shepard Interpolation

Avaldsnes

Interpolating the seismic data with Shepard's produced a "grainy" or "coarser" image. Comparing all three grid sizes (figures 35, 36 and 37), 0.1 by 0.1 m grid had the best resolution and details. There are more reflections in the seismic image and minimum loss of data. In grids – 0.25 by 0.25 m and 0.5 by 0.5 m – the absence of seismic data is due to the fact that the subbottom profiler got stuck and that particular inline and crossline shows that. The shipwreck is easily identifiable in the inline of all the three grids because it makes a synclinal shape in the seismic image. However, in the crosslines and time slices, this becomes

more challenging. However, by zooming out of the seismic image it is slightly easier to identify the shipwreck in the crossline. Zooming out the seismic image a bit makes it a bit easier to identify the shipwreck in the crossline. The shipwreck makes the same bowl shape but it's more laterally extensive. In the time slice, the outline can be identified by distribution of the amplitudes. The shipwreck outline makes an elongated shape in the time slice.

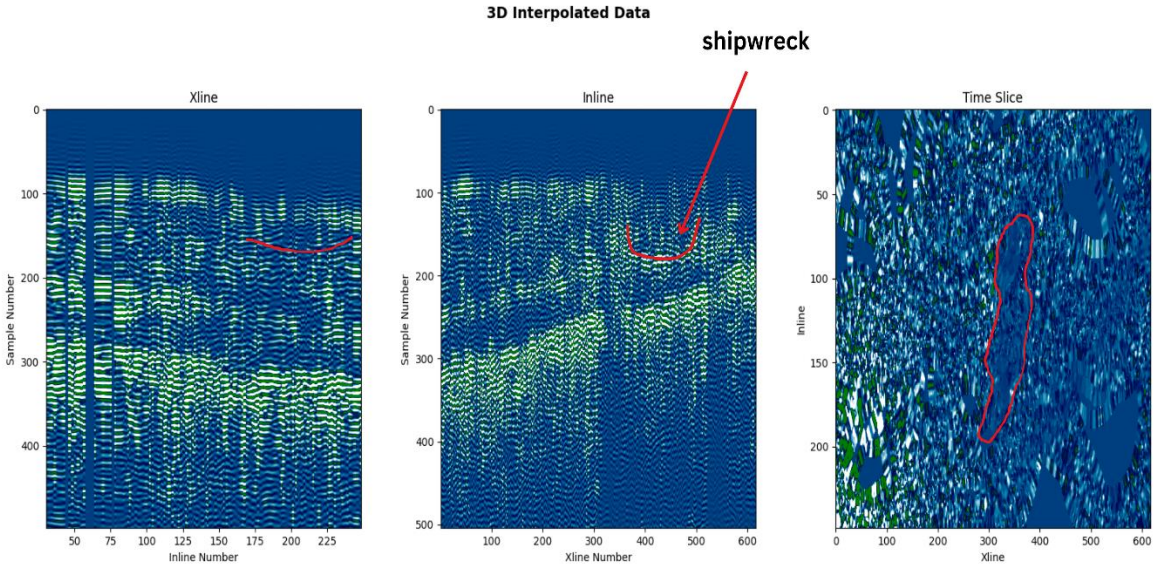

Figure 35 0.1 by 0.1 m grid size Shepard's interpolation result in Avaldsnes

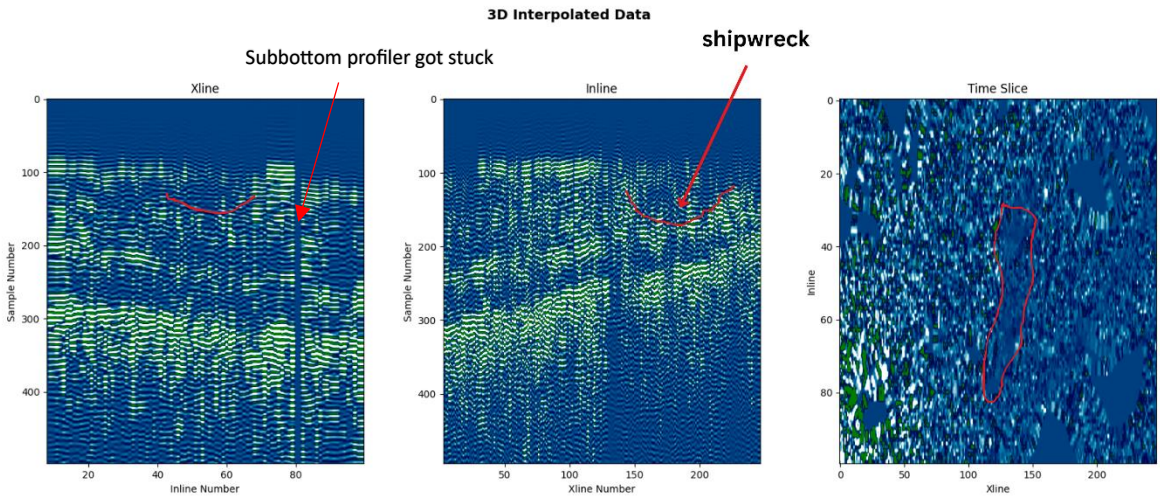

Figure 36 0.25 by 0.25 m grid size Shepard's interpolation result in Avaldsnes

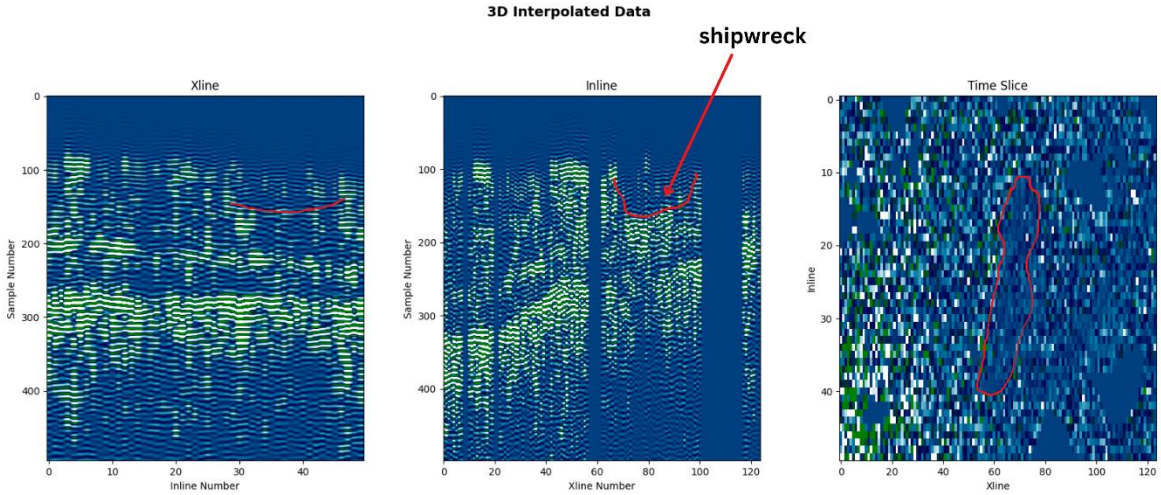

Figure 37 0.5 by 0.5 m grid size Shepard's interpolation result in Avaldsnes

Hafrsfjord

Envelope

All three interpolated seismic images (figures 38, 39 and 40) have the "coarse" texture. However, there is an increase in smoothing with increasing grid size. The shipwreck in Hafrsfjord is easily identifiable because of the "bump" it produces in the seismic image. In the time slice, the shipwreck has more of a round distortion. To expand on this, the 0.1 by 0.1 m grid size shows the highest resolution and the 0.5 by 0.5 m grid size has the lowest resolution with the shipwreck almost impossible to identify in the inline and crossline.

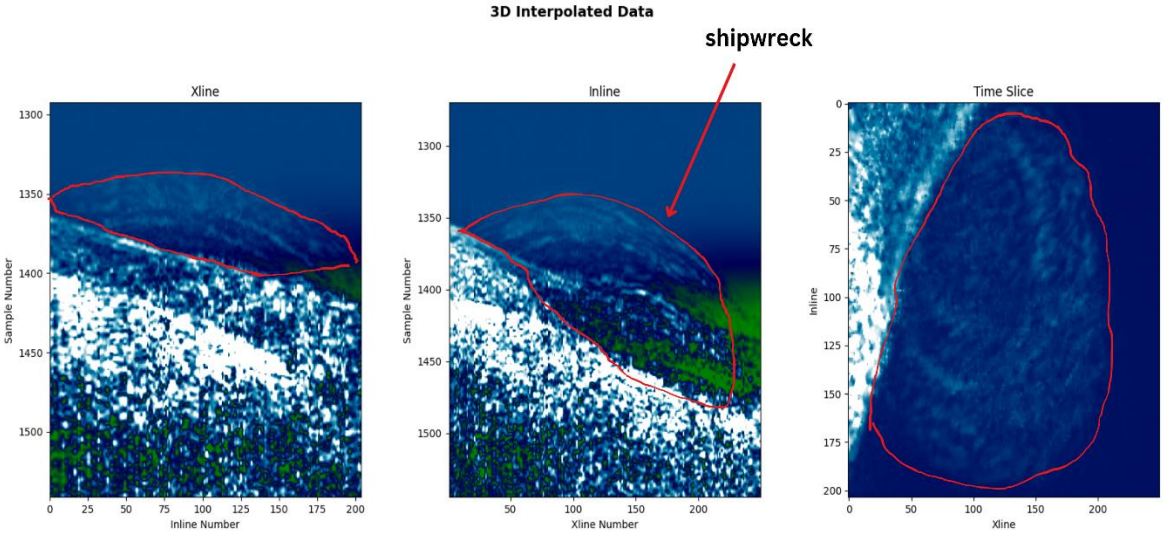

Figure 38 0.1 by 0.1 m grid size Shepard's interpolation result in Hafrsfjord

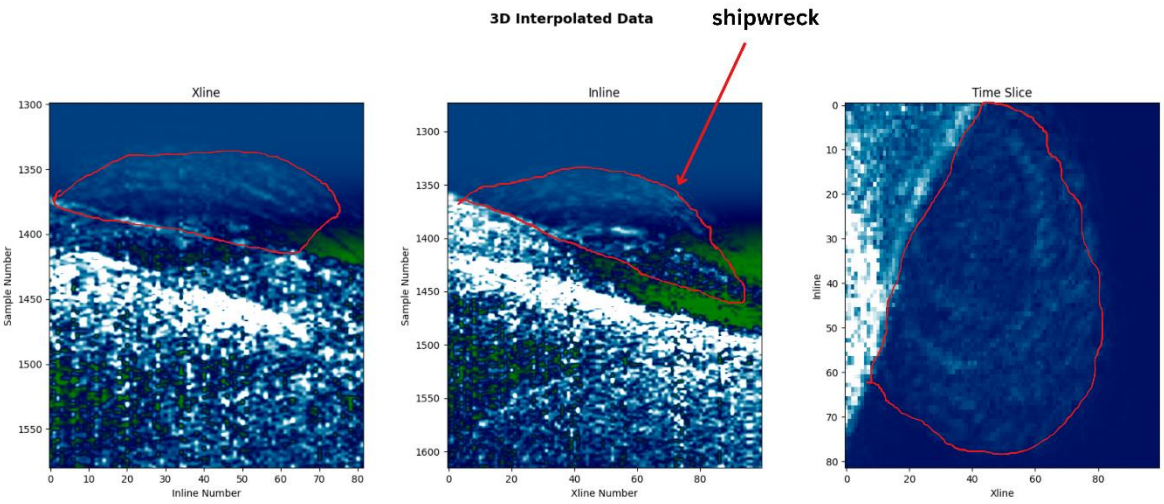

Figure 39 0.25 by 0.25 m grid size Shepard's interpolation result in Hafrsfjord

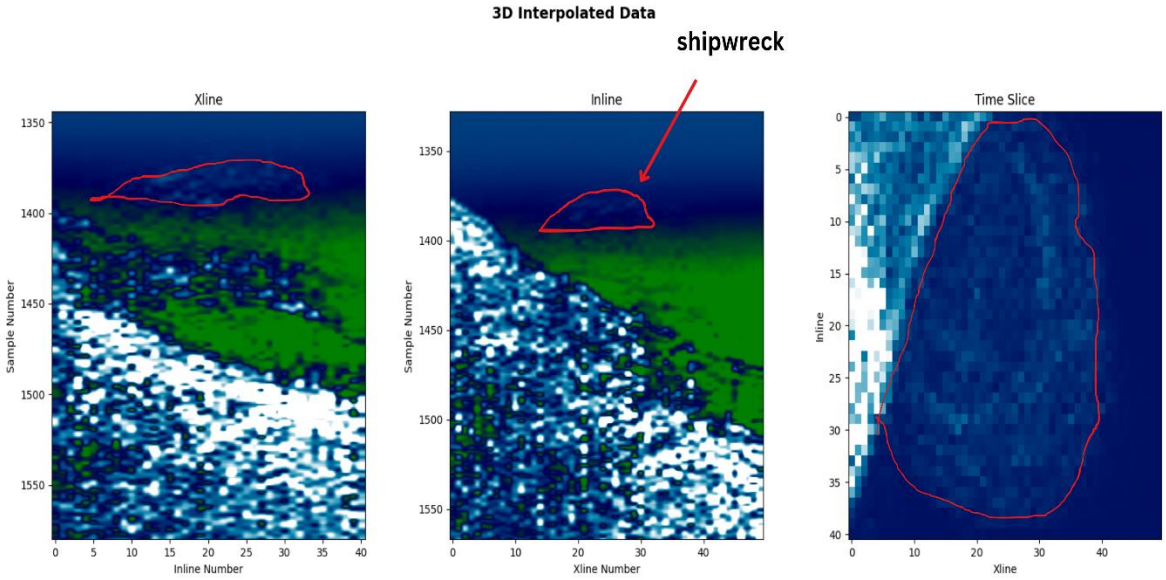

Figure 40 0.5 by 0.5 m grid size Shepard's interpolation result in Hafrsfjord

Fullwave

The shipwreck outline is easier to identify (figures 41, 42 and 43) when interpolated with Shepard's method. The 'graininess' of the seismic image make it easy to identify the extent and shipwreck outline. However, the challenge of identifying the shipwreck in the time slice still persists.

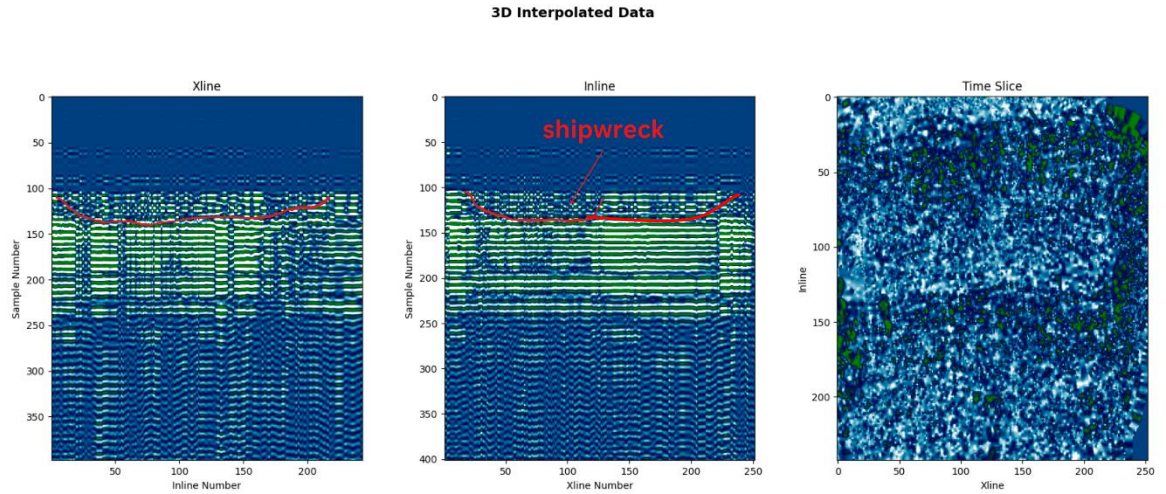

Figure 41 0.1 by 0.1 m grid size Shepard's interpolation result in Hafrsfjord (fullwave)

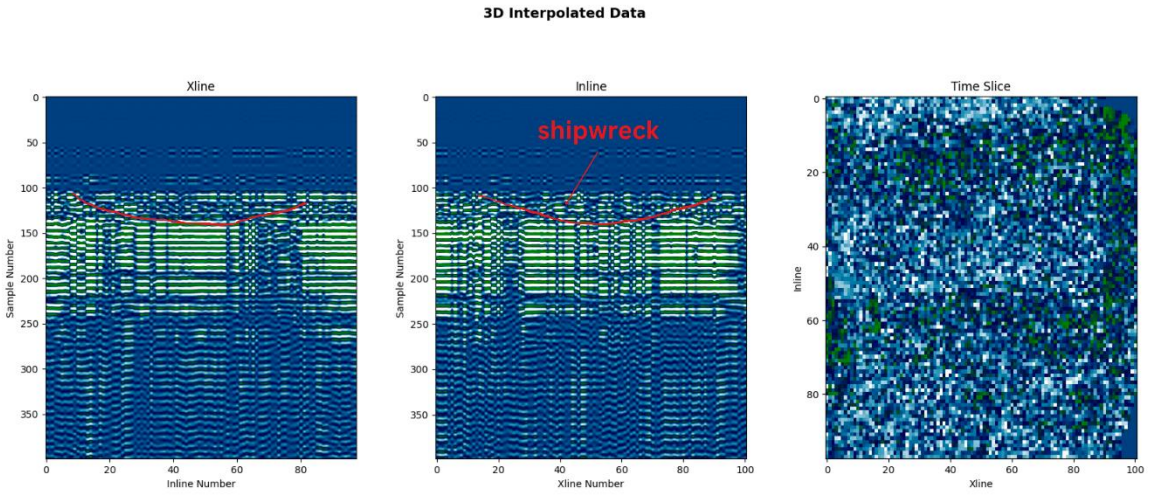

Figure 42 0.25 by 0.25 m grid size Shepard's interpolation result in Hafrsfjord (fullwave)

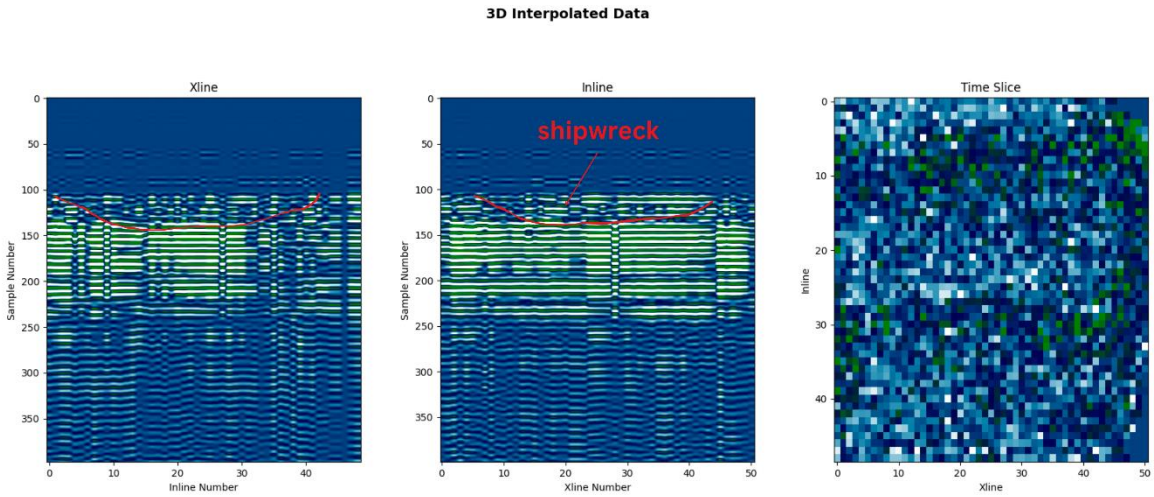

Figure 43 0.5 by 0.5 m grid size Shepard's interpolation result in Hafrsfjord (fullwave)

Cubic Interpolation Verses Shepard's Interpolation

Cubic interpolation has a greater smoothing effect on the seismic data than Shepard's interpolation. Furthermore, the smoothing effect makes it difficult to identify the shipwreck's outline. This is made easy with Shepard's interpolation but comes with the risk of not being able to identify the shipwreck with increasing grid size. That's the advantage of using Shepard's interpolation over cubic interpolation. However, the disadvantage they have in common is the difficulty of identifying the shipwreck in the crosslines. The difficulty might also have something to do with the orientation of the shipwreck in and on the seafloor compared to the survey geometry.

Migration

Migration After Cubic Interpolation

Avaldsnes

Migrating the seismic data with a 20° and 40° aperture, the results show little difference. In the 0.1 by 0.1 m grid size (figures 44 and 45), the migrated seismic data look similar, however, comparing the crosslines shows reflections to be dipping when migrated with a 20° aperture but do not with a 40° aperture. In addition, reflections in the 0.25 by 0.25 m grid size 20° migrated seismic data (figures 46 and 47) have more consistent reflections but do not when migrated with 40°. In figures 48 and 49, the 0.5 by 0.5 m grid size, it is difficult to find any differences. This might be due to the large grid size. Overall, because of the shallow waters in Avaldsnes, the tested aperture sizes do not make a big difference in the migrated seismic images. The outline of the shipwreck differs in all three grid sizes. The 0.1 by 0.1 m grid size closely resembles the smooth bottom of the ship compared to the other two grid sizes. The shipwreck takes on a more synclinal shape in the inlines. The outlines in the crosslines are more consistent, but are difficult to interpretate because of how the reflections from the shipwreck match with other reflections. Finally, the outline of the ship can be seen in the time slice and increasing grid size has the resolution go from smooth to "grainy".

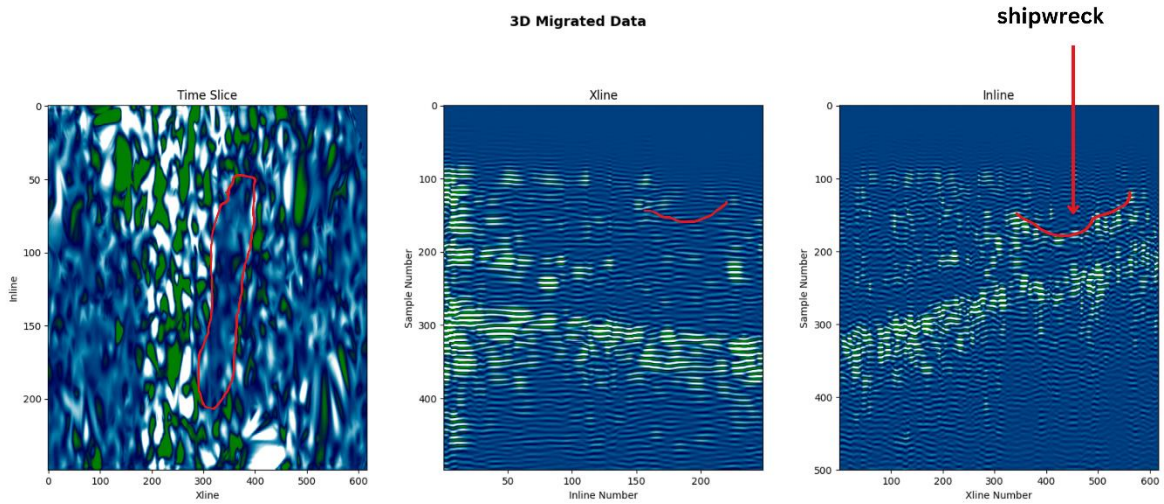

Figure 44 Migrated cubic interpolated seismic data (0.1 by 0.1 m grid size) with 20 degree aperture in Avaldsnes

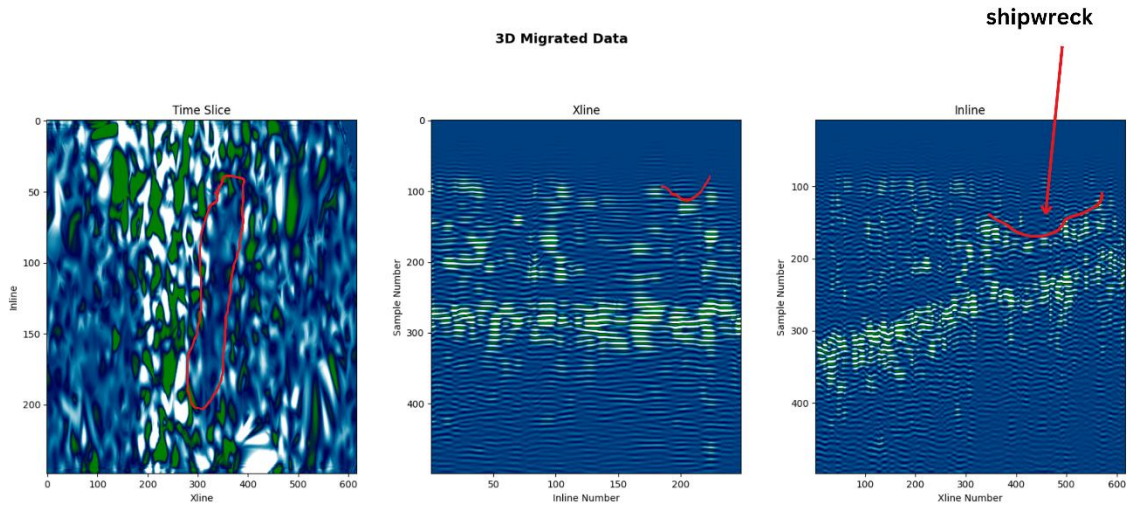

Figure 45 Migrated cubic interpolated seismic data (0.1 by 0.1 m grid size) with 40 degree aperture in Avaldsnes

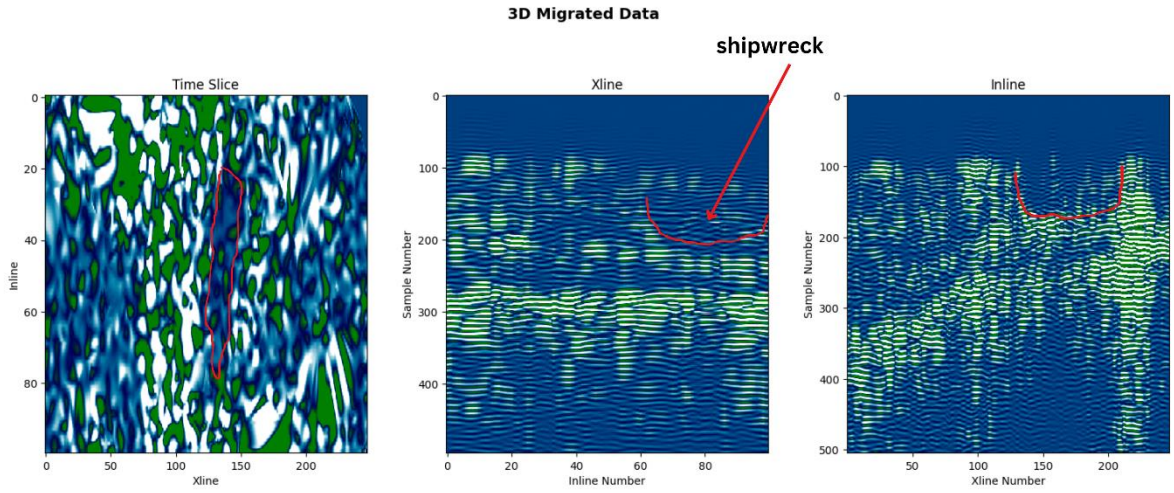

Figure 46 Migrated cubic interpolated seismic data (0.25 by 0.25 m grid size) with 20 degree aperture in Avaldsnes

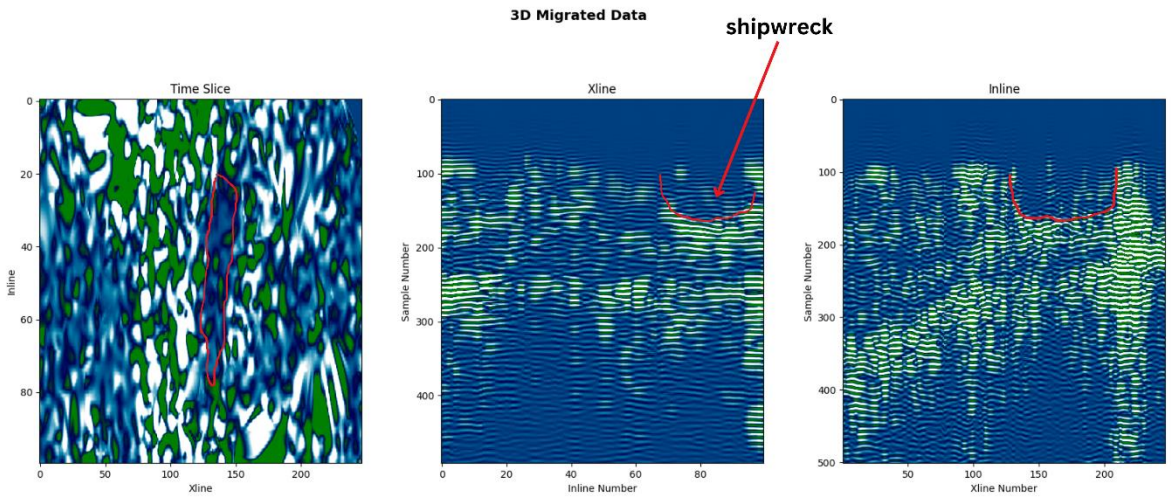

Figure 47 Migrated cubic interpolated seismic data (0.25 by 0.25 m grid size) with 40 degree aperture in Avaldsnes

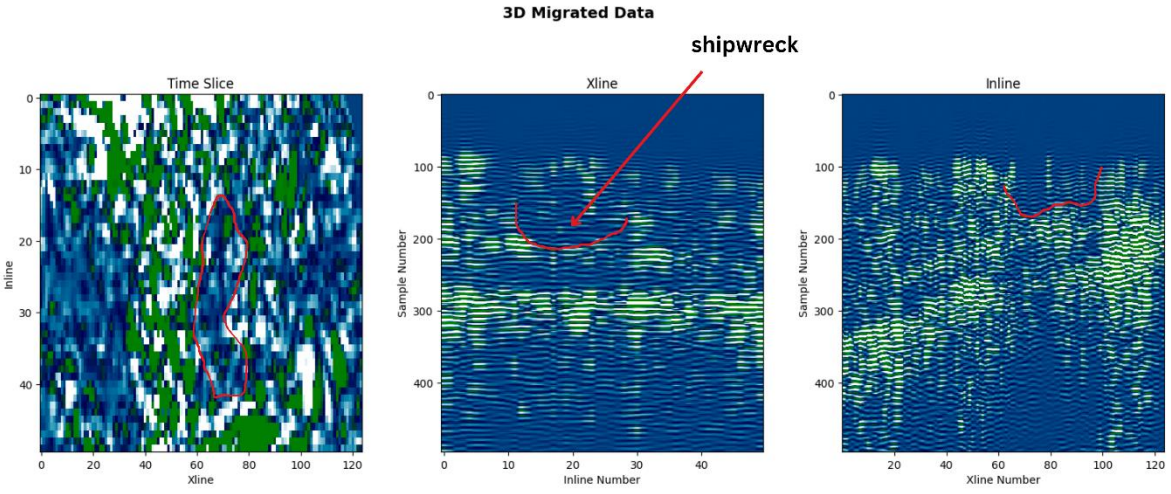

Figure 48 Migrated cubic interpolated seismic data (0.5 by 0.5 m grid size) with 20 degree aperture in Avaldsnes

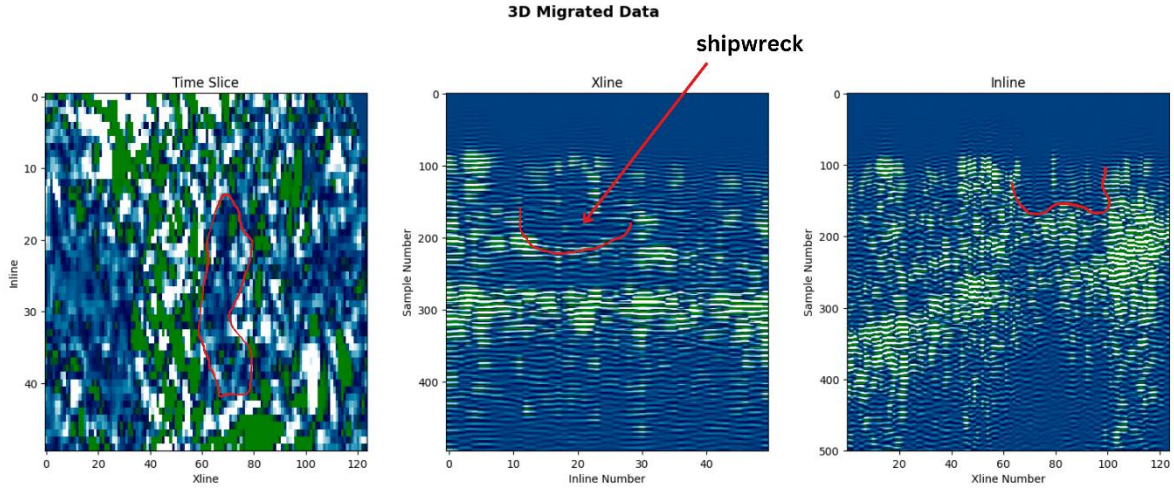

Figure 49 Migrated cubic interpolated seismic data (0.5 by 0.5 m grid size) with 40 degree aperture in Avaldsnes

Hafrsfjord

Envelope

In Hafrsfjord, migrating with a 20° aperture produces better results in imaging the shipwreck and reflections. Additionally, in all seismic images (figure 50 to 55), the shipwreck can be identified. All migrated seismic images with 20° aperture migration are sharper, has less noise and smoothing. In addition, dipping events or reflections are destroyed with a wider migration aperture. In figure 52, steeping events are present, however, when migrated with 40° aperture, these are no longer present (figure 53). In addition, the greater aperture size causes more smoothing of reflections. Overall, the 20° aperture size produces a better migrated result than migrating with 40° aperture. The shipwreck outline in the time slice is somewhat similar to the 3D model shipwreck's outline (figure 56). It is close enough but still not clear to know if that's a shipwreck or not.

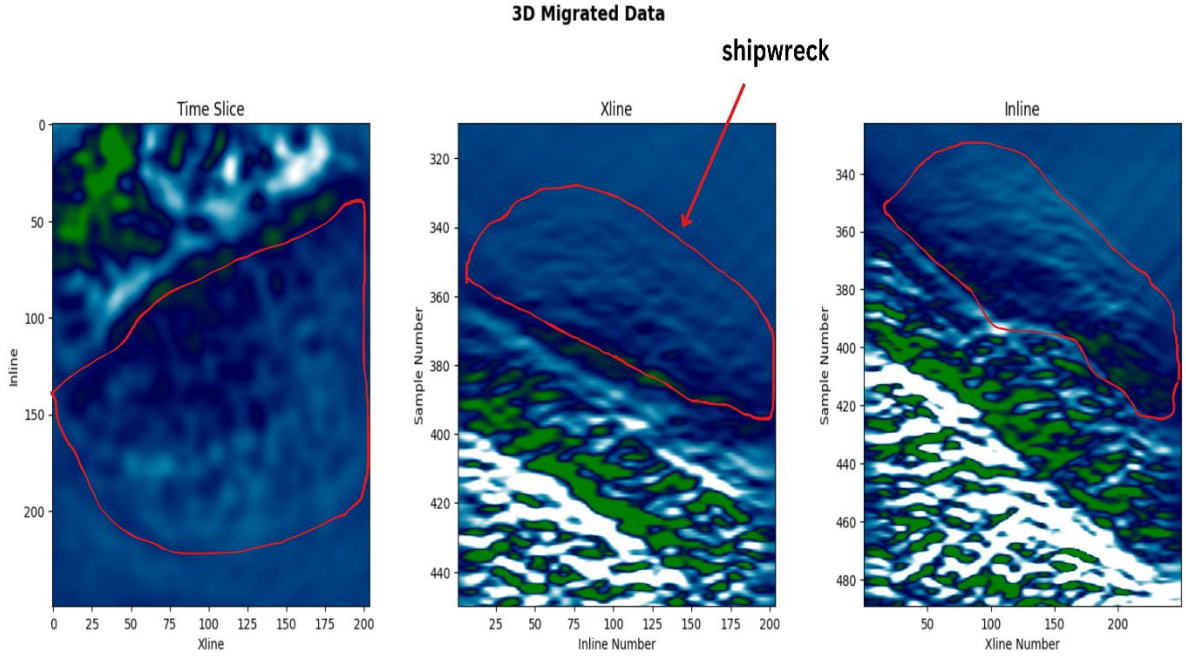

Figure 50 Migrated cubic interpolated seismic data (0.1 by 0.1 m grid size) with 20 degree aperture in Hafrsfjord

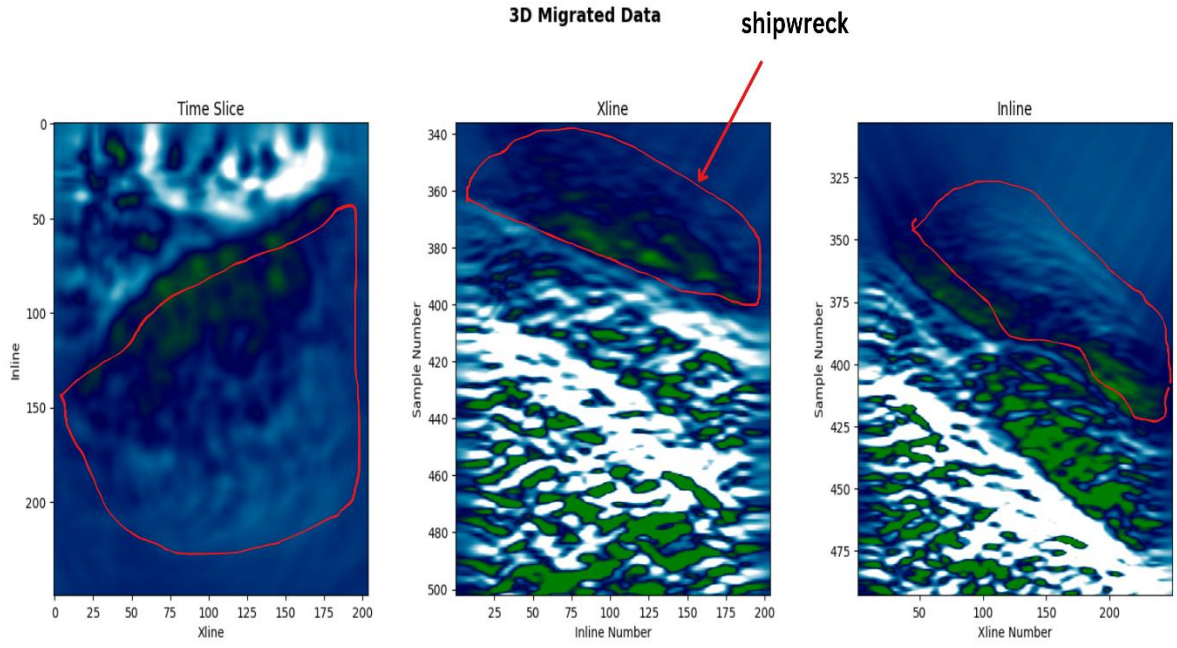

Figure 51 Migrated cubic interpolated seismic data (0.1 by 0.1 m grid size) with 40 degree aperture in Hafrsfjord

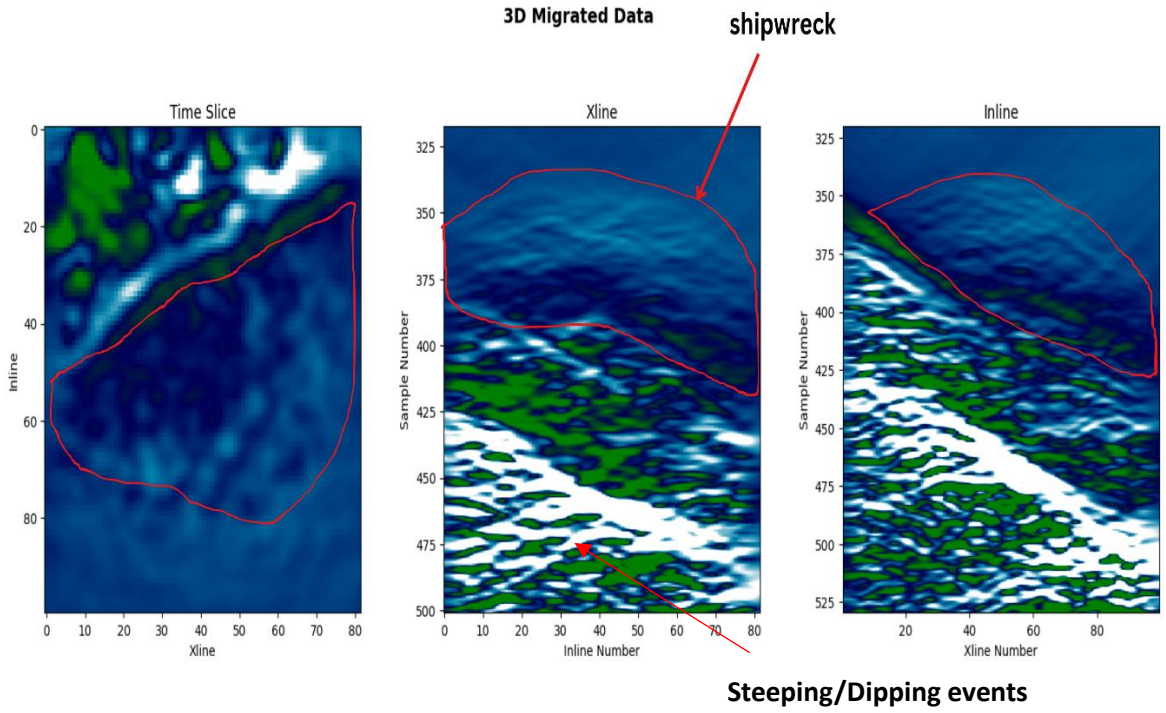

Figure 52 Migrated cubic interpolated seismic data (0.25 by 0.25 m grid size) with 20 degree aperture in Hafrsfjord

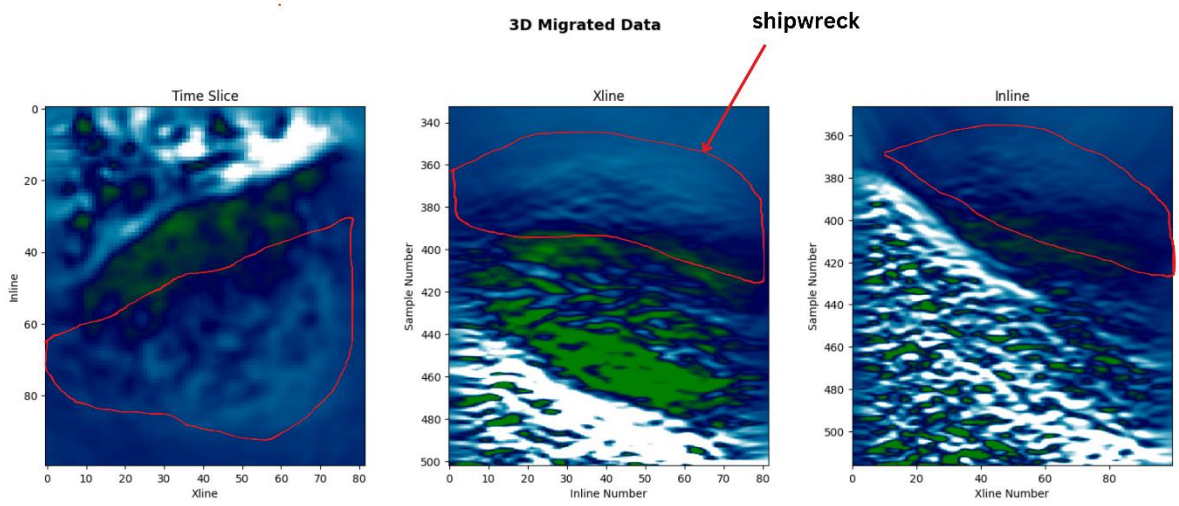

Figure 53 Migrated cubic interpolated seismic data (0.25 by 0.25 m grid size) with 40 degree aperture in Hafrsfjord

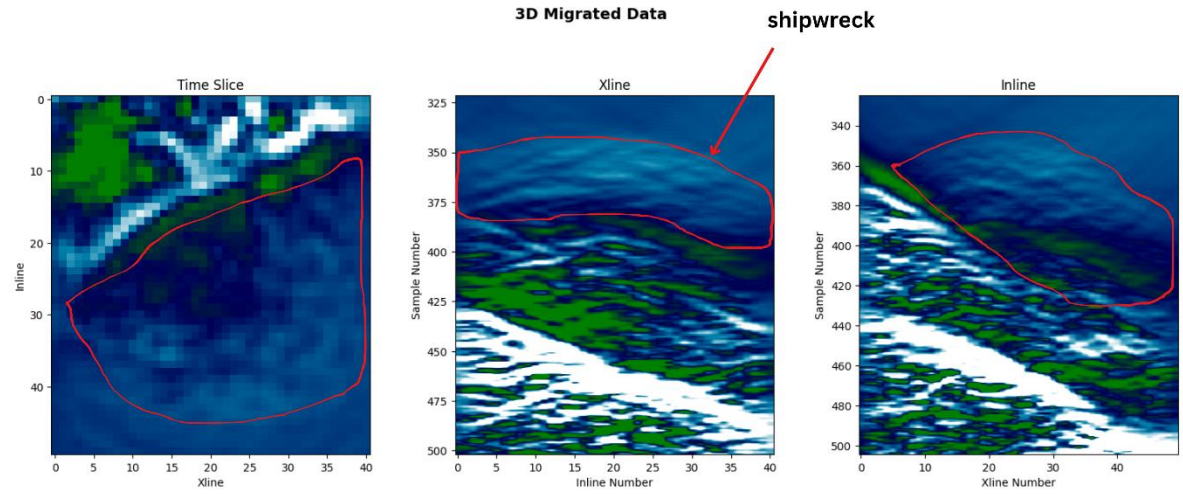

Figure 54 Migrated cubic interpolated seismic data (0.5 by 0.5 m grid size) with 20 degree aperture in Hafrsfjord

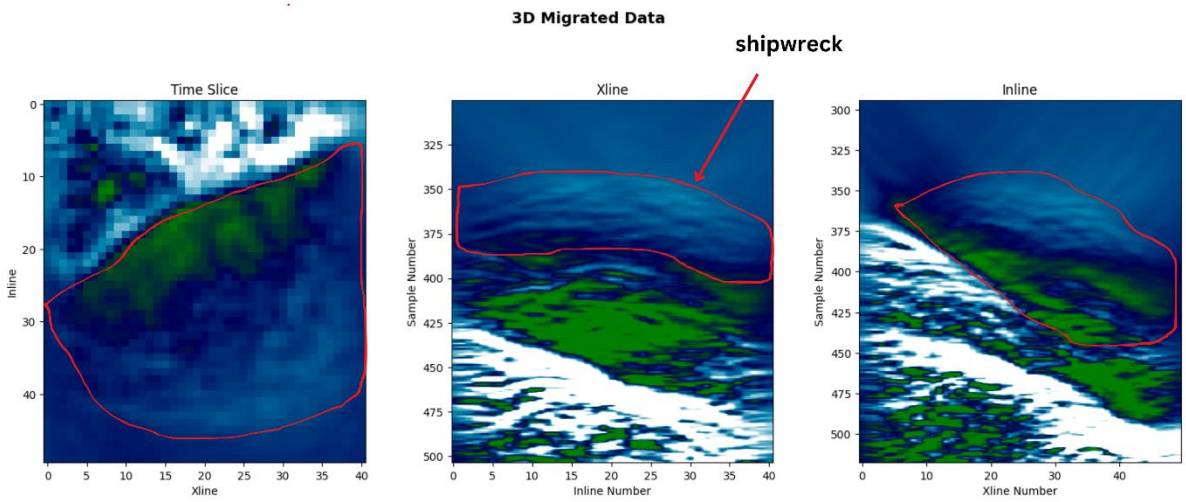

Figure 55 Migrated cubic interpolated seismic data (0.5 by 0.5 m grid size) with 40 degree aperture in Hafrsfjord

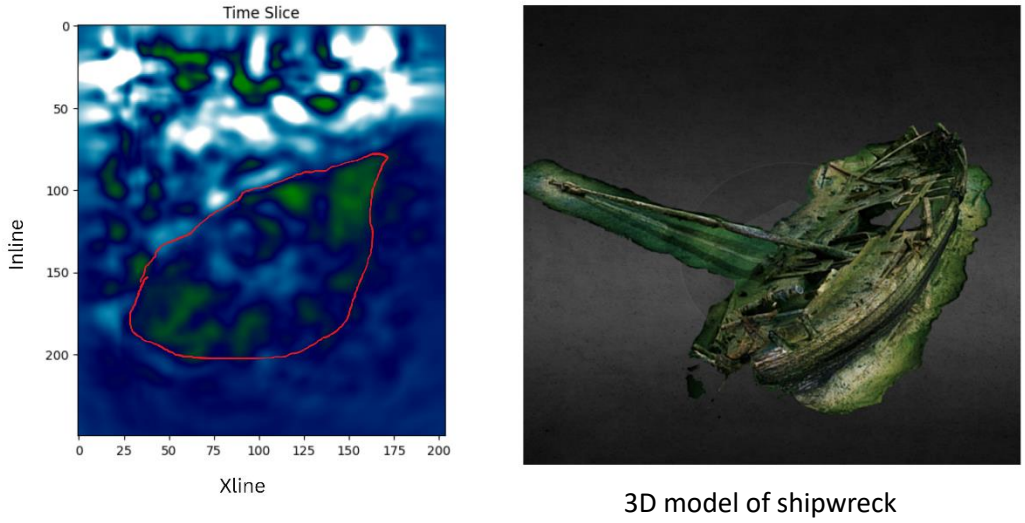

Figure 56 Comparison of time slice (left) and 3D model of the shipwreck in Hafrsfjord (right)

Fullwave

Figures 57 to 62 show little to no difference migrating with a 20º or 40º aperture size. The shipwreck and its extent become more challenging to identify. The shipwreck does not make the synclinal shape observed in figures 32, 33, 34, 41, 42 and 43 after migration. The shape is more flat and almost parallel to the horizontal reflections. Furthermore, the shipwreck was not identifiable in the time slice even after migration.

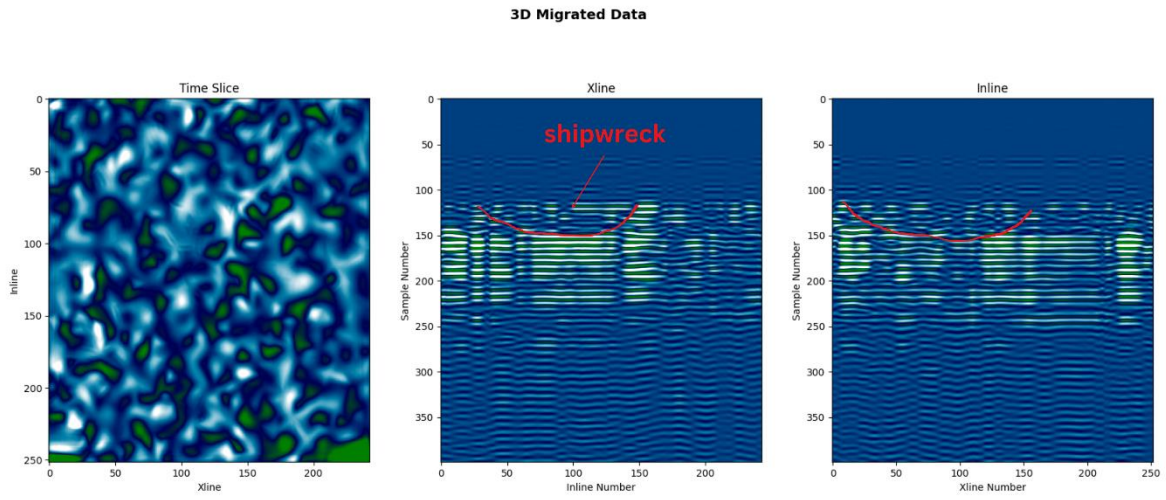

Figure 57 Migrated cubic interpolated seismic data (0.1 by 0.1 m grid size) with 20 degree aperture in Hafrsfjord (fullwave)

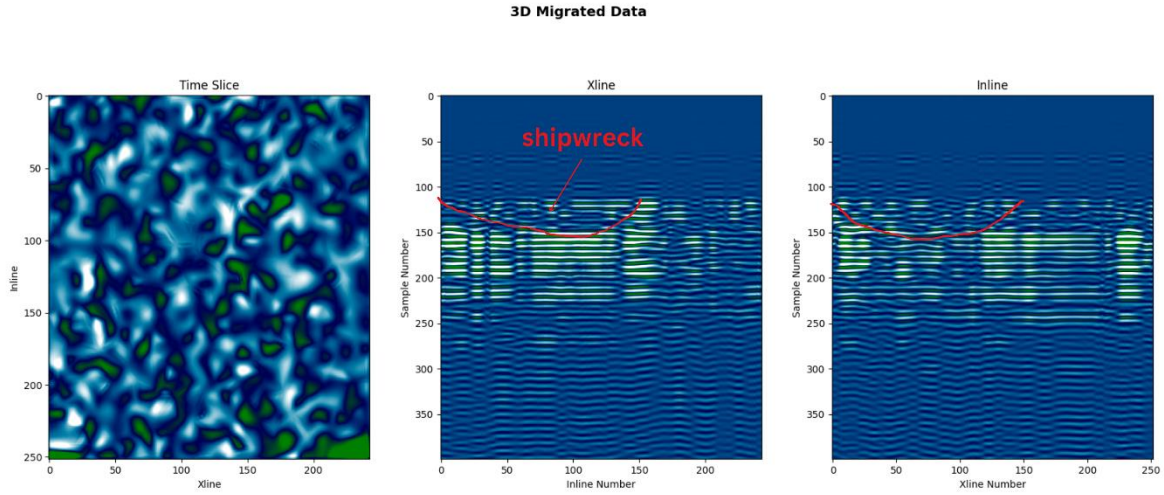

Figure 58 Migrated cubic interpolated seismic data (0.1 by 0.1 m grid size) with 40 degree aperture in Hafrsfjord (fullwave)

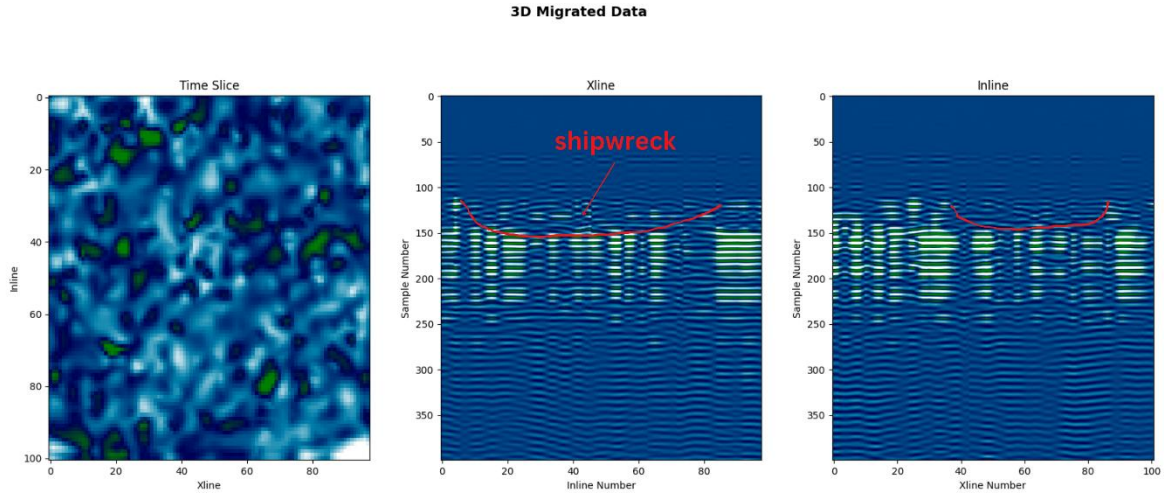

Figure 59 Migrated cubic interpolated seismic data (0.25 by 0.25 m grid size) with 20 degree aperture in Hafrsfjord (fullwave)

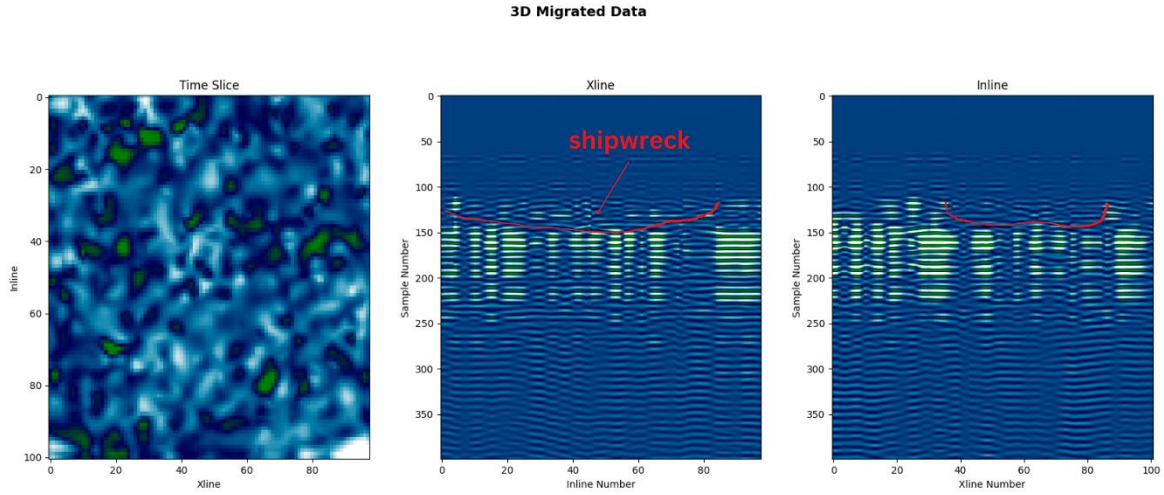

Figure 60 Migrated cubic interpolated seismic data (0.25 by 0.25 m grid size) with 40 degree aperture in Hafrsfjord (fullwave)

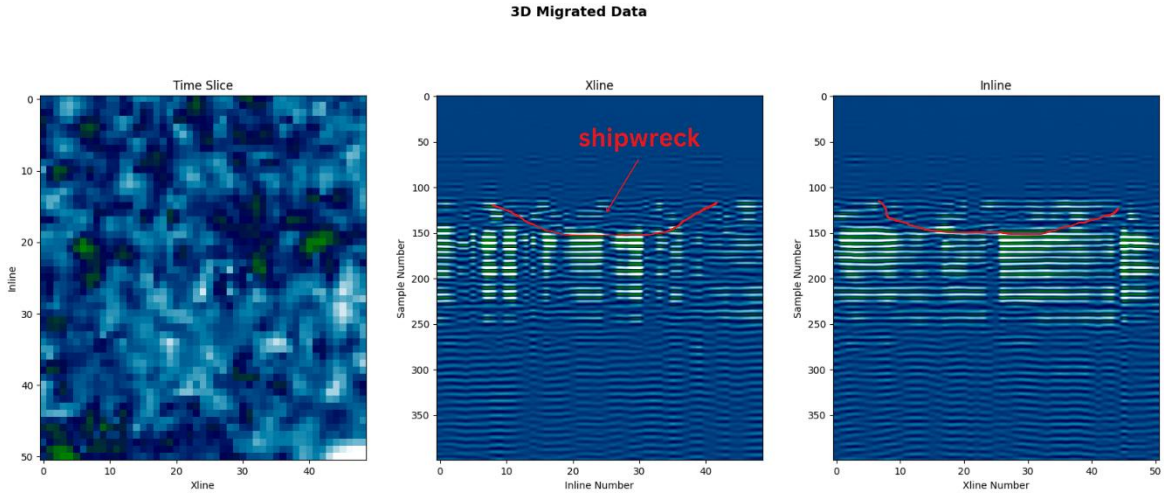

Figure 61 Migrated cubic interpolated seismic data (0.5 by 0.5 m grid size) with 20 degree aperture in Hafrsfjord (fullwave)

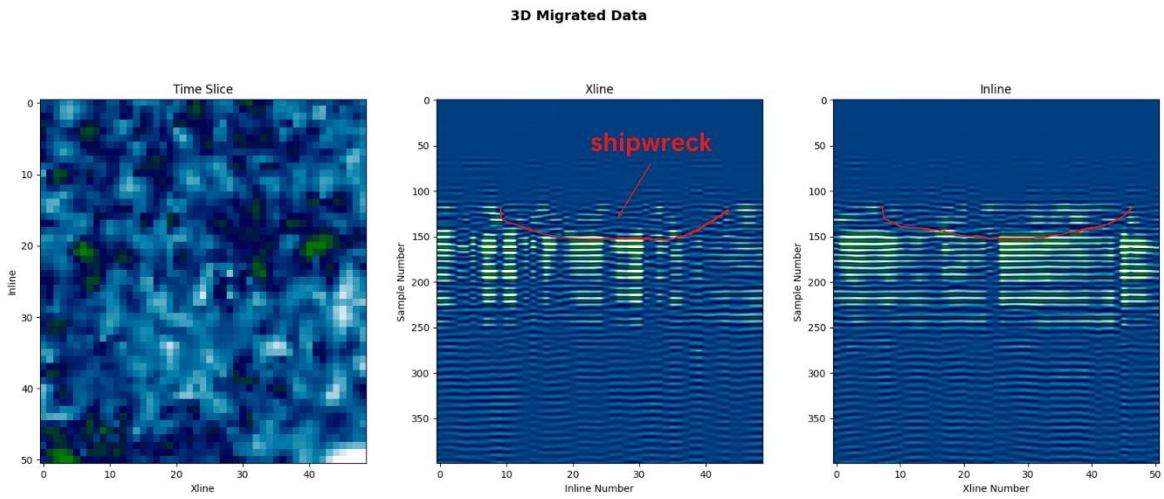

Figure 62 Migrated cubic interpolated seismic data (0.5 by 0.5 m grid size) with 40 degree aperture in Hafrsfjord (fullwave)

Migration After Shepard's Interpolation

Avaldsnes

Migration after Shepard's interpolation with aperture sizes 20° and 40° show little difference (figures 63 to 68). Reflections have a slightly higher amplitude in 0.1 by 0.1 m grid size with 20° than 40° aperture. The other results show no difference. As mentioned earlier, this might be due the shallow waters in Avaldsnes where the tested aperture size does not affect migration results.

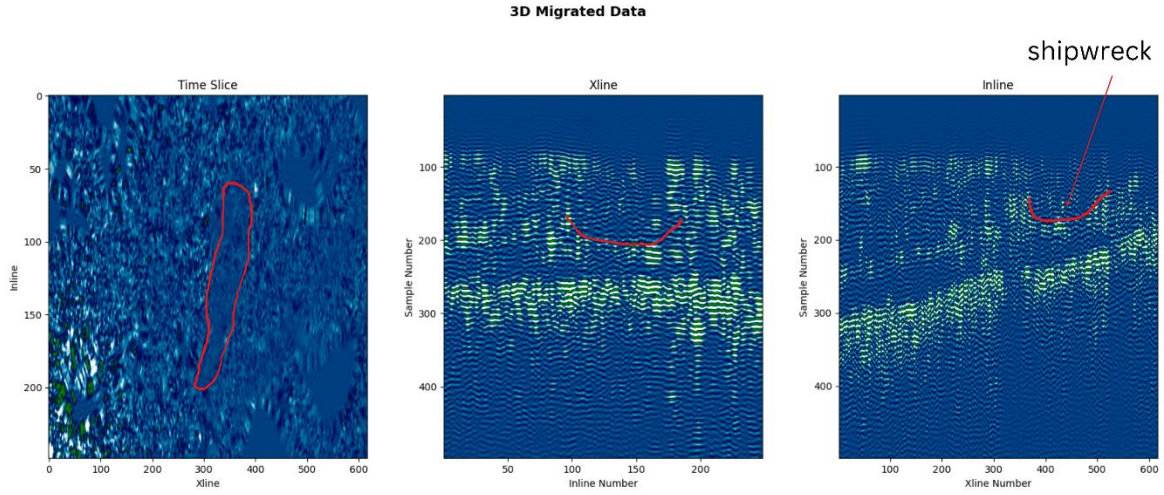

Figure 63 Migrated Shepard's interpolated seismic data (0.1 by 0.1 m grid size) with 20 degree aperture in Avaldsnes

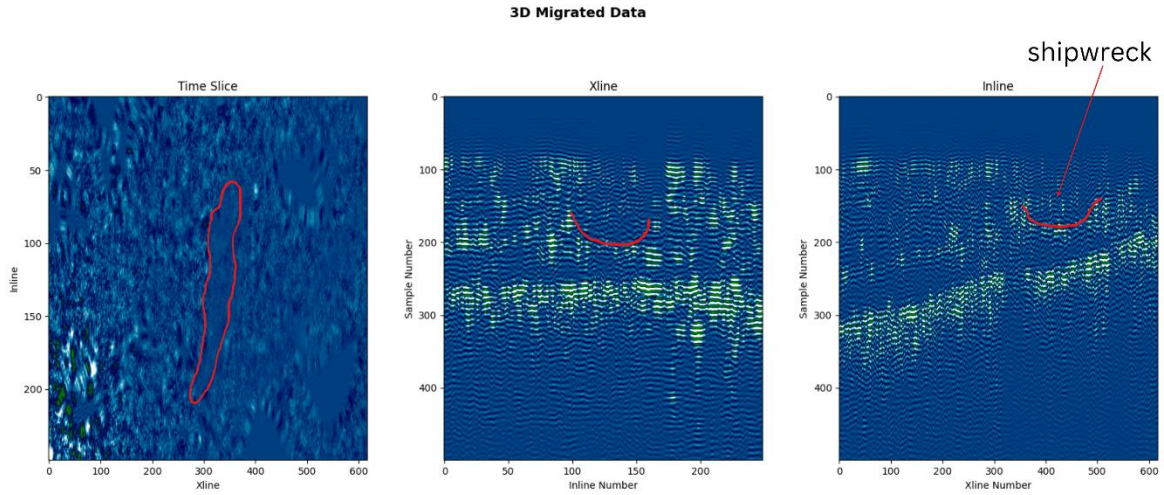

Figure 64 Migrated Shepard's interpolated seismic data (0.1 by 0.1 m grid size) with 40 degree aperture in Avaldsnes

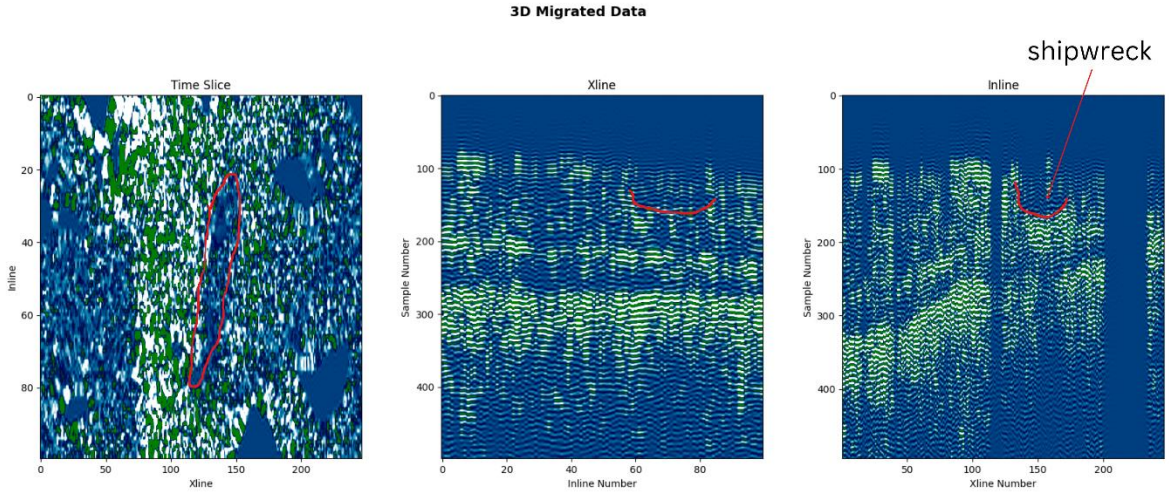

Figure 65 Migrated Shepard's interpolated seismic data (0.25 by 0.25 m grid size) with 20 degree aperture in Avaldsnes

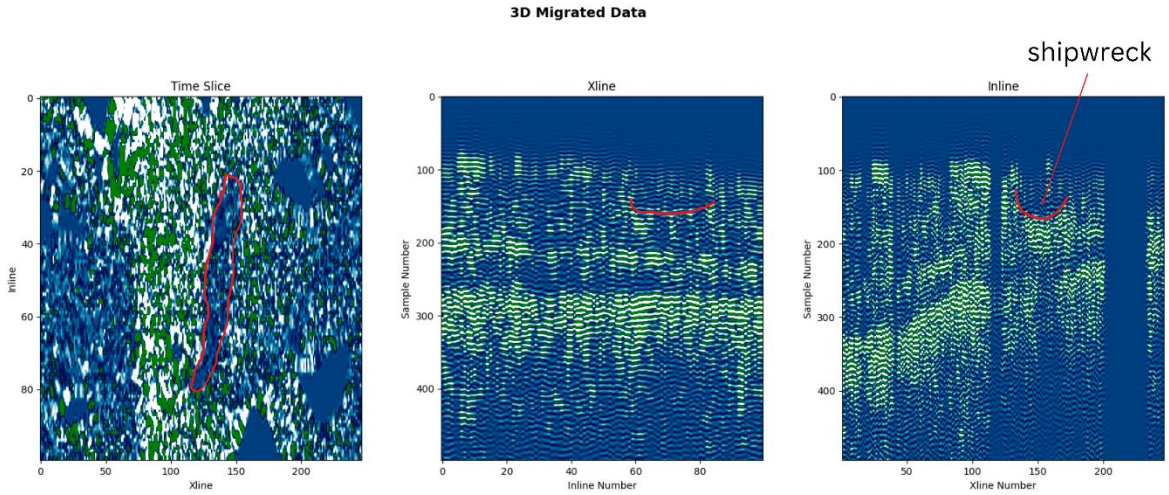

Figure 66 Migrated Shepard's interpolated seismic data (0.25 by 0.25 m grid size) with 40 degree aperture in Avaldsnes

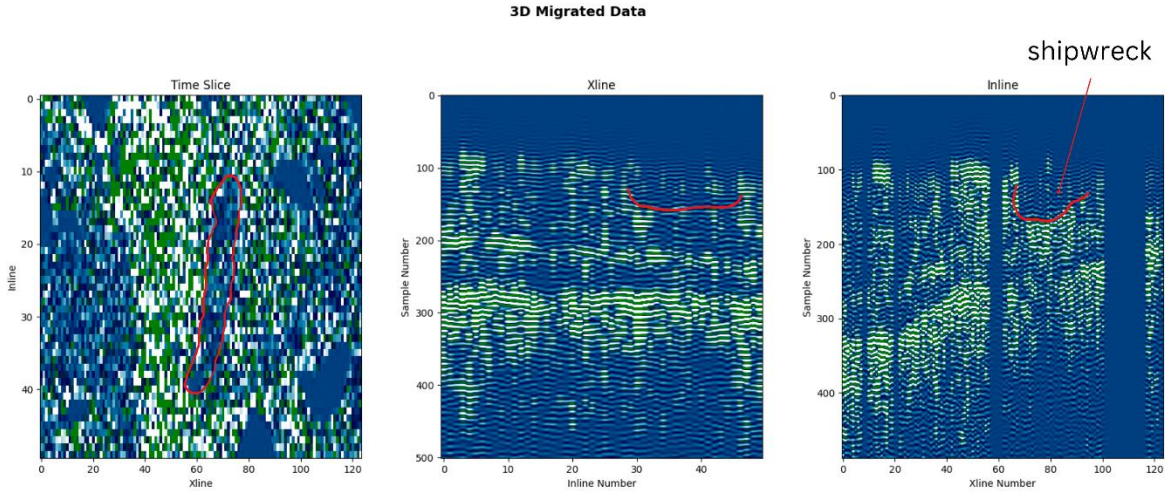

Figure 67 Migrated Shepard's interpolated seismic data (0.5 by 0.5 m grid size) with 20 degree aperture in Avaldsnes

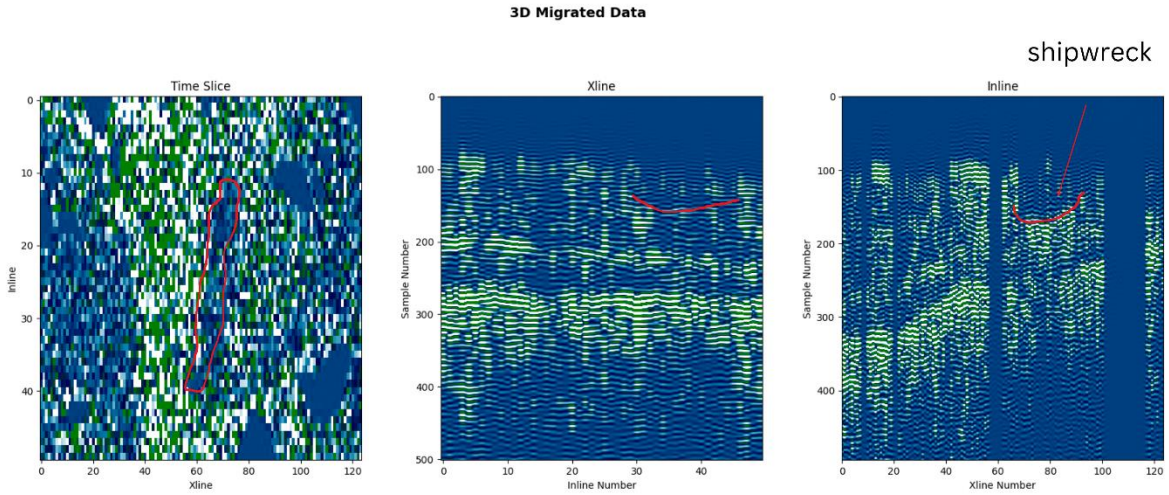

Figure 68 Migrated Shepard's interpolated seismic data (0.5 by 0.5 m grid size) with 40 degree aperture in Avaldsnes

Hafrsjord

Envelope

In Hafrsfjord, aperture size affects the migrated seismic data due to the depth of the water column being approximately 40 m. Migrating with 20° aperture size causes a considerable amount of smoothing (figures 69, 71 and 73), migrating with 40° aperture has less smoothness and more graininess (figures 70, 72 and 74). Furthermore, reflections are more obvious in 40° migrated seismic data. Identifying the shipwreck outline was somewhat

difficult in the inline and crosslines. In the interpolated results, the shipwreck was an obvious bump and a distorted image. However, after migration although the shipwreck still appears as a bump it is not obvious to the eye. The shipwreck outline is obvious in the time slice because it closely resembles a ship. The shipwreck's outline is much closer to the 3D model of the shipwreck after migrating seismic data with Shepard's interpolation (figure 75). The outline is clearly shown - is lying in the same direction as the 3D image - and the surrounded lines could be the shipwreck's mast, which is difficult to say because small or thin objects at this water depths are difficult to observe. Furthermore, the middle of the shipwreck corresponds to the middle of the 3D model shipwreck, which could be a cargo room.

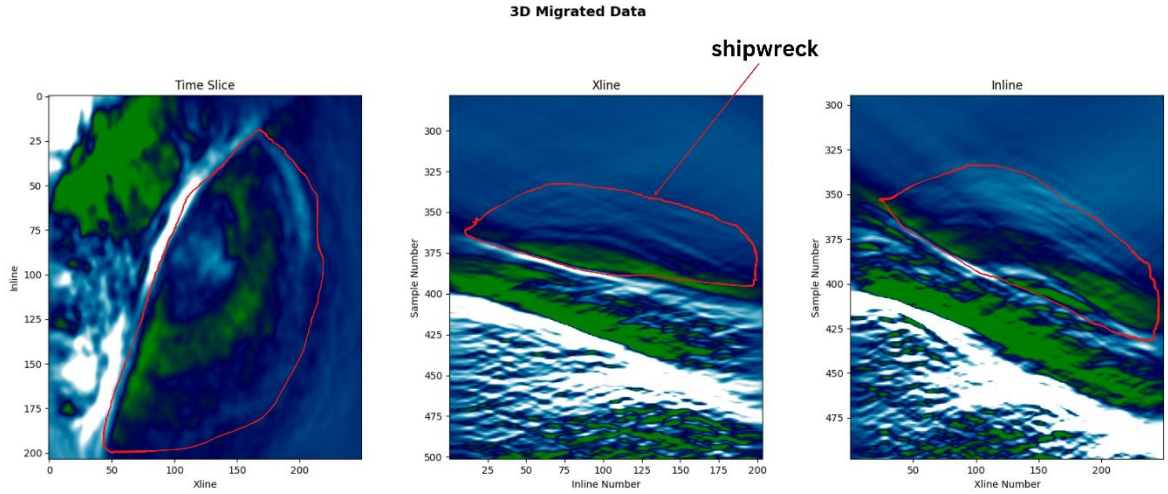

Figure 69 Migrated Shepard's interpolated seismic data (0.1 by 0.1 m grid size) with 20 degree aperture in Hafrsfjord

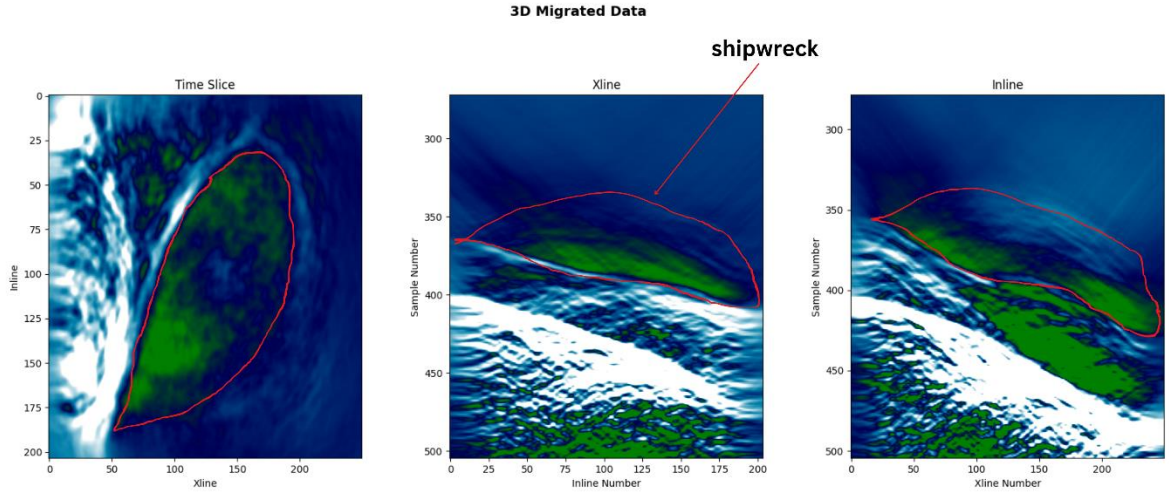

Figure 70 Migrated Shepard's interpolated seismic data (0.1 by 0.1 m grid size) with 40 degree aperture in Hafrsfjord

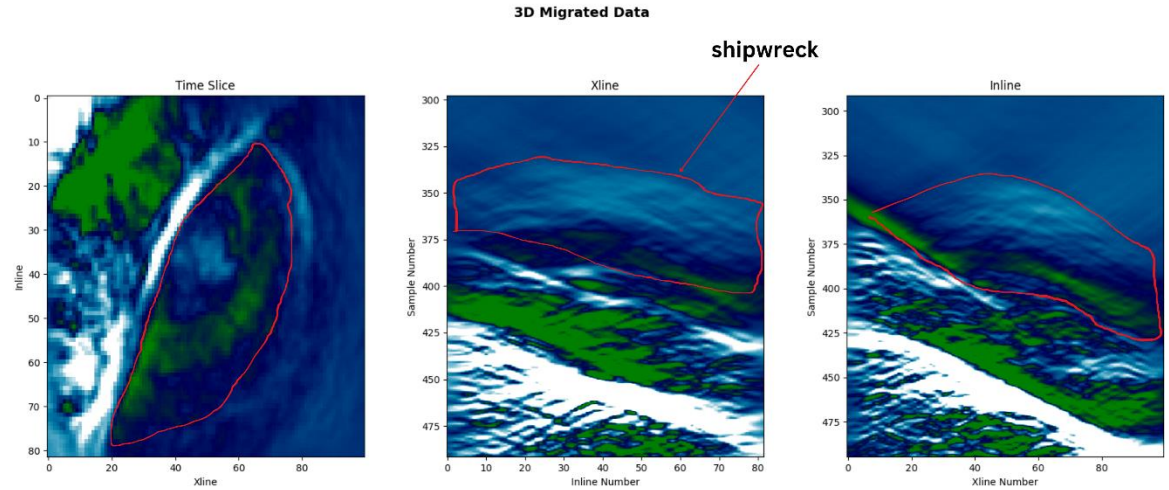

Figure 71 Migrated Shepard's interpolated seismic data (0.25 by 0.25 m grid size) with 20 degree aperture in Hafrsfjord

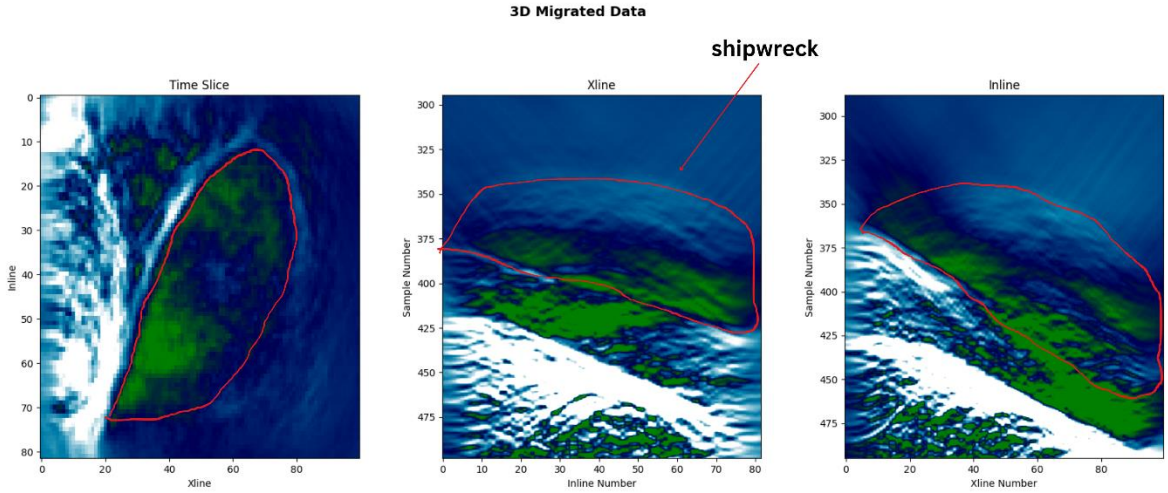

Figure 72 Migrated Shepard's interpolated seismic data (0.25 by 0.25 m grid size) with 40 degree aperture in Hafrsfjord

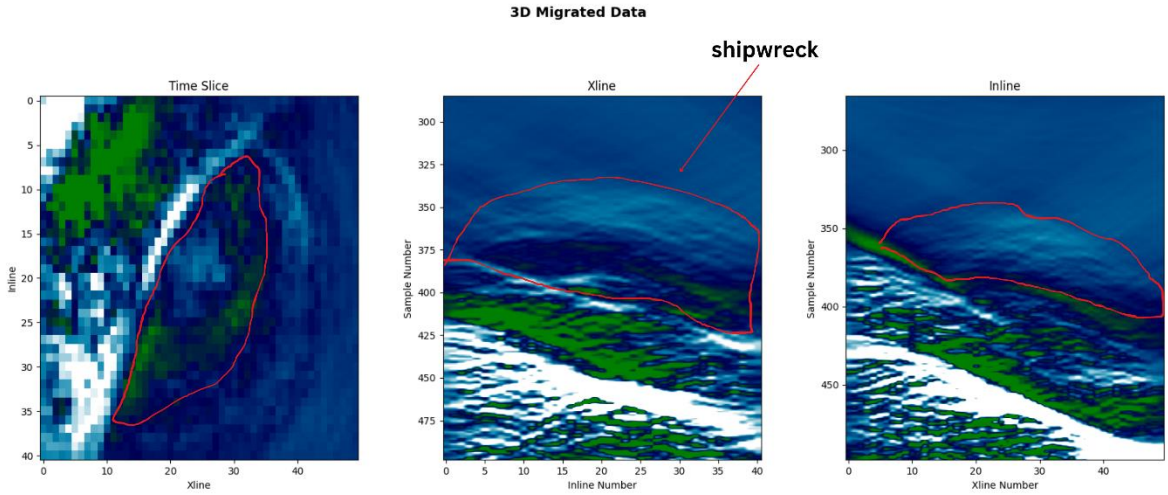

Figure 73 Migrated Shepard's interpolated seismic data (0.5 by 0.5 m grid size) with 20 degree aperture in Hafrsfjord

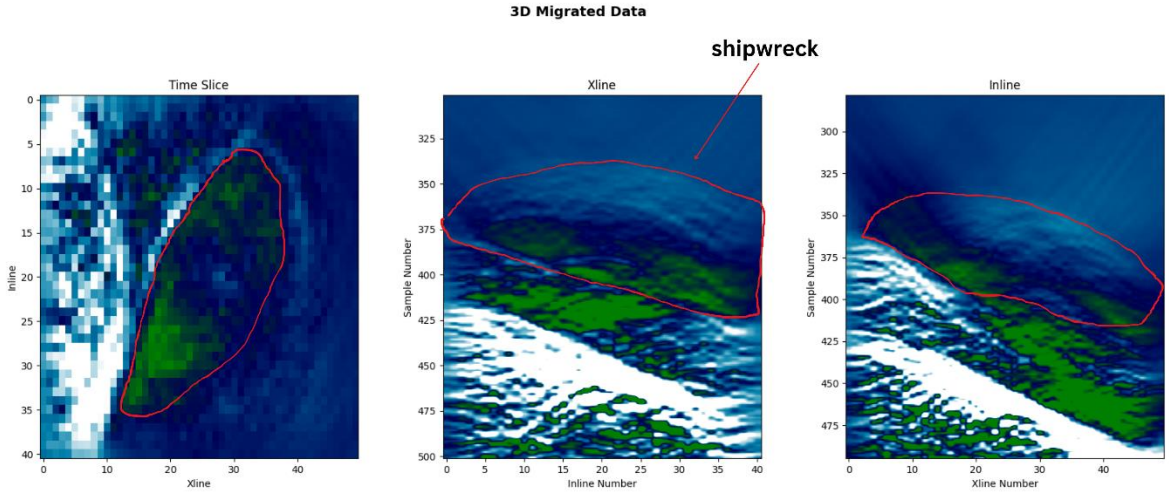

Figure 74 Migrated Shepard's interpolated seismic data (0.5 by 0.5 m grid size) with 40 degree aperture in Hafrsfjord

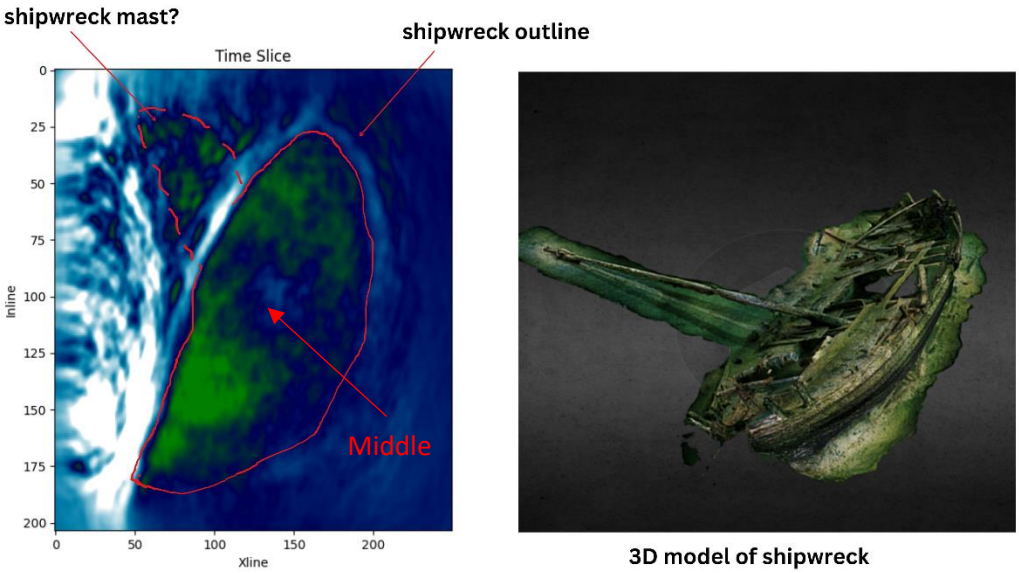

Figure 75 Comparison of shipwreck in time slice (left) and the 3D model of shipwreck (right)

Fullwave

The shipwreck becomes increasingly difficult to identify when migrated after Shepard's interpolation (figures 76 to 80). The reflections become increasingly grainy and discontinuous making it difficult to identify the actual shipwreck extent and outline. The same is true in the time slice which was not possible to identify the shipwreck Furthermore, the tested aperture size does not affect the seismic images.

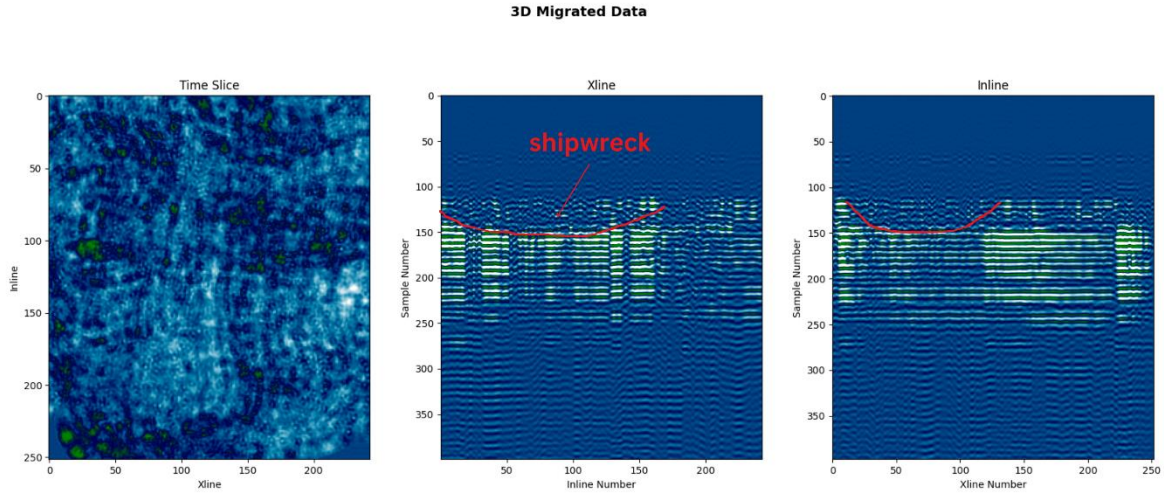

Figure 76 Migrated Shepard's interpolated seismic data (0.1 by 0.1 m grid size) with 20 degree aperture in Hafrsfjord (fullwave)

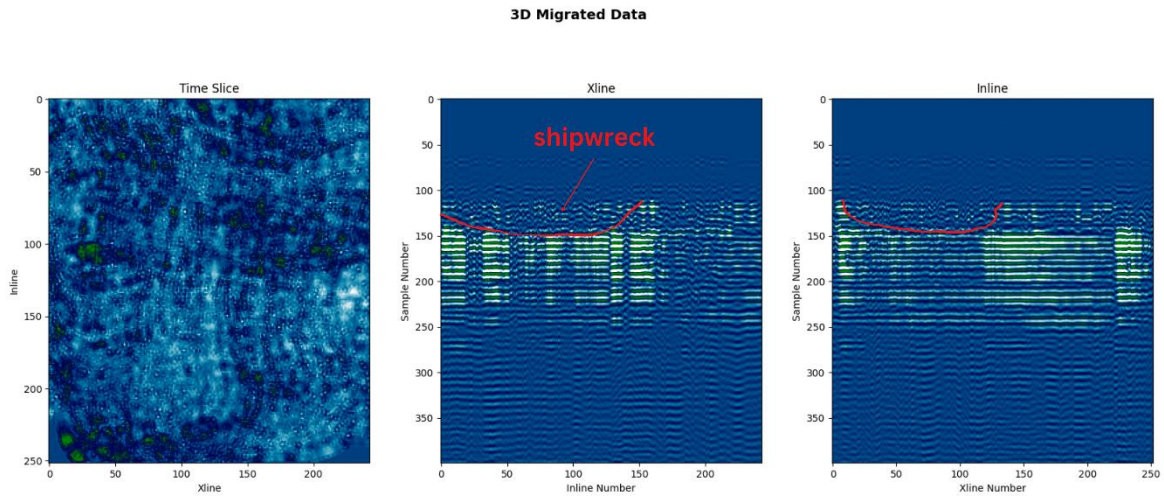

Figure 77 Migrated Shepard's interpolated seismic data (0.1 by 0.1 m grid size) with 40 degree aperture in Hafrsfjord (fullwave)

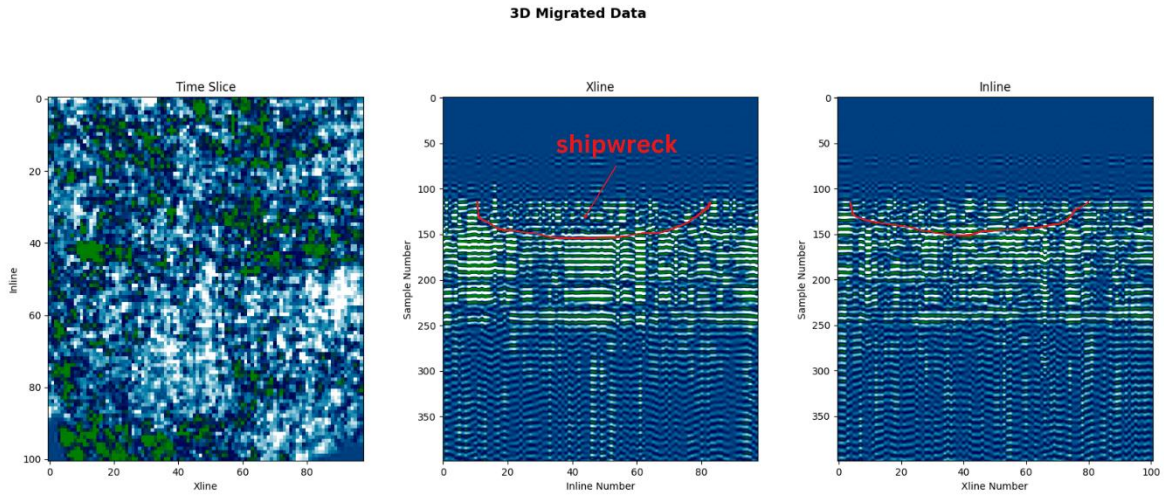

Figure 78 Migrated Shepard's interpolated seismic data (0.25 by 0.25 m grid size) with 20 degree aperture in Hafrsfjord (fullwave)

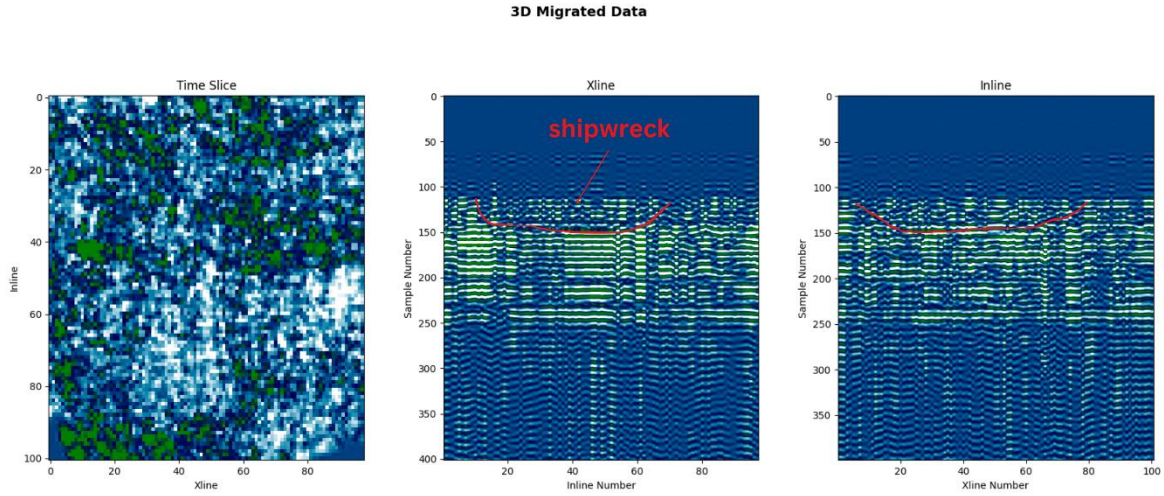

Figure 79 Migrated Shepard's interpolated seismic data (0.25 by 0.25 m grid size) with 40 degree aperture in Hafrsfjord (fullwave)

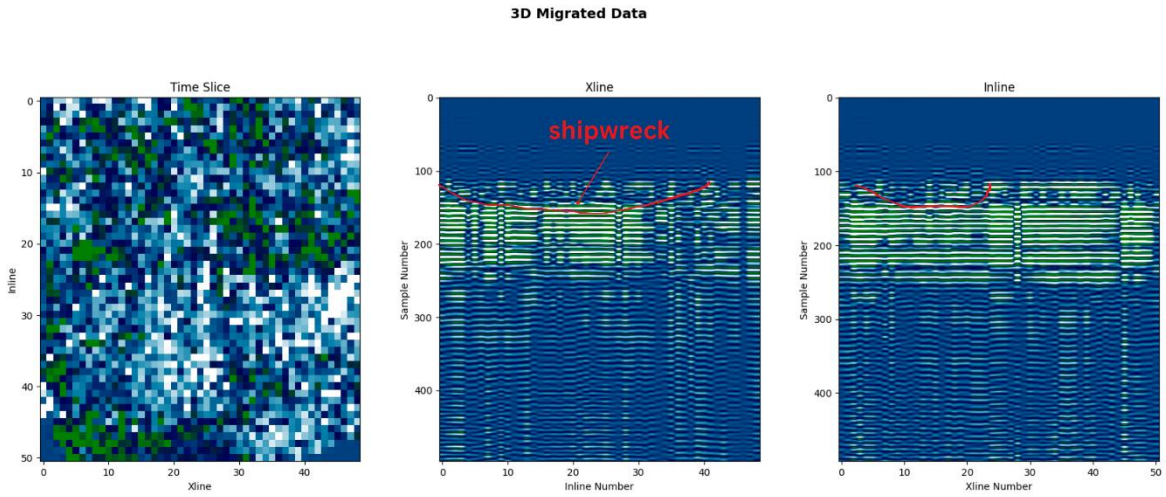

Figure 80 Migrated Shepard's interpolated seismic data (0.5 by 0.5 m grid size) with 20 degree aperture in Hafrsfjord (fullwave)

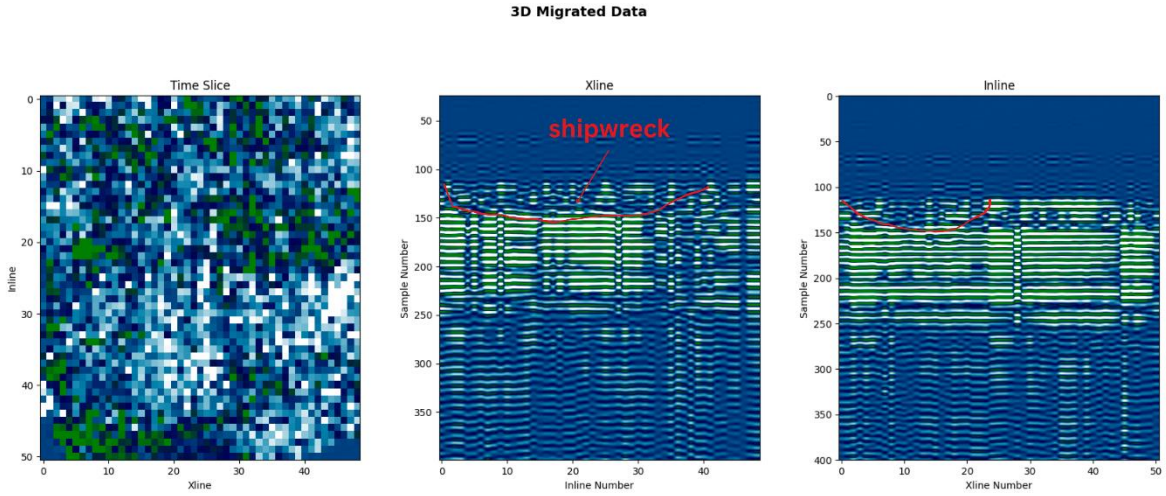

Figure 81 Migrated Shepard's interpolated seismic data (0.5 by 0.5 m grid size) with 40 degree aperture in Hafrsfjord (fullwave)

Cubic Interpolation Versus Shepard's Interpolation For Migration

Migrating the seismic data with Shepard's interpolation produces better results over cubic interpolation. Seismic images do not have considerable amount of smoothing and are more "grainy" or "coarse". This makes it easy to identify reflections of the shipwreck in the seismic image.

Conclusions

The objectives outlined below in the thesis were achieved:

i) Test various interpolation methods for interpolating an irregular dataset to a regular dataset
ii) Investigate the optimal interpolation techniques on two different cases
iii) Assess the quality from the interpolation and migration method.

A regular 3D grid was created, seismic data was interpolated using the 3D grid with two interpolation methods tested (cubic and Shepard's) and the interpolated seismic results were migrated with Stolt's method. To conclude:

- Using a grid size of 0.1 by 0.1 m median binned seismic data interpolated Shepard's method produced the best results. The tested aperture size has no effect on the quality of migration if seismic data was acquired in shallow waters (<2m). However, aperture size affects migrated results when acquired in fairly deep waters with the best tested aperture size to be 40^{o}.
- Cubic interpolation has the disadvantage of over smoothing the seismic data making it difficult to identify artifacts. The smoothing effect becomes prominent in Shepard's interpolation with increasing grid size. Therefore, keeping the grid size small eliminates most of this effect. The shipwrecks in Avaldsnes and Hafrsfjord (envelope) were imaged properly and easily identifiable. Although, in Avaldsnes there were some challenges in identifying the shipwreck in the crosslines.
- Comparing envelope and fullwave data acquired in Hafrsfjord. The envelope data proved to be more robust and provided better seismic images for interpretation.

Overall, results were satisfactory. To further improve on this, various sampling rates, increase of data density, acquiring crossline data in Avaldsnes and using Kirchoff migration can be tested.

References

Aki, K., & Richards, P. G. (2002). *Quantitative seismology*.

Arnott, S. H., Dix, J. K., Best, A. I., & Gregory, D. J. (2005). Imaging of buried archaeological materials: the reflection properties of archaeological wood. *Marine Geophysical Researches*, *26*, 135-144.

Baradello, L., & Carcione, J. M. (2008). Optimal seismic-data acquisition in very shallow waters: Surveys in the Venice lagoon. *Geophysics*, *73*(6), Q59-Q63.

Bates, M. R., Bates, C. R., & Briant, R. M. (2007). Bridging the gap: a terrestrial view of shallow marine sequences and the importance of the transition zone. *Journal of Archaeological Science*, *34*(9), 1537-1551.

Bull, J. M., Gutowski, M., Dix, J. K., Henstock, T. J., Hogarth, P., Leighton, T. G., & White, P. R. (2005). Design of a 3D Chirp sub-bottom imaging system. *Marine Geophysical Researches*, *26*, 157-169.

Bull, J. M., Quinn, R., & Dix, J. K. (1998). Reflection coefficient calculation from marine high resolution seismic reflection (Chirp) data and application to an archaeological case study. *Marine Geophysical Researches*, *20*, 1-11.

Chopra, S., Castagna, J., & Portniaguine, O. (2006). Seismic resolution and thin-bed reflectivity inversion. *CSEG recorder*, *31*(1), 19-25.

Grimm, O. (2011). A maritime-archaeological analysis of Hafrsfjord–seen from the land side. *Tverrfaglige Perspektiver*, *2*, 23-33.

Grøn, O., & Boldreel, L. O. (2014). Chirping for large-scale maritime archaeological survey: a strategy developed from a practical experience-based approach. *Journal of Archaeology*, *2014*.

Grøn, O., Boldreel, L. O., Cvikel, D., Kahanov, Y., Galili, E., Hermand, J.-P., Nævestad, D., & Reitan, M. (2015). Detection and mapping of shipwrecks embedded in sea-floor sediments. *Journal of Archaeological Science: Reports*, *4*, 242-251.

GRØN[1], O., JØRGENSEN, A. N., & HOFFMANN, G. (2007). Marine archaeological survey by high-resolution sub-bottom profilers.

Imposa, S., Grassi, S., Di Raimondo, S., Patti, G., Lombardo, G., & Panzera, F. (2018). Seismic refraction tomography surveys as a method for voids detection: an application to the archaeological park of Cava Ispica, Sicily, Italy. *International Journal of Architectural Heritage*, *12*(5), 806-815.

Jaijel, R., Kanari, M., Glover, J. B., Rissolo, D., Beddows, P. A., Ben-Avraham, Z., & Goodman-Tchernov, B. N. (2018). Shallow geophysical exploration at the ancient maritime Maya site of Vista Alegre, Yucatan Mexico. *Journal of Archaeological Science: Reports*, *19*, 52-63.

Janowski, L., Kubacka, M., Pydyn, A., Popek, M., & Gajewski, L. (2021). From acoustics to underwater archaeology: deep investigation of a shallow lake using high-resolution hydroacoustics—the case of Lake Lednica, Poland. *Archaeometry*, *63*(5), 1059-1080.

Kartverket. (2023). kartverket.no

McCarthy, J., Benjamin, J., Winton, T., & Van Duivenvoorde, W. (2019). The rise of 3D in maritime archaeology. *3D Recording and Interpretation for Maritime Archaeology*, 1-10.

Micallef, A. (2011). Marine geomorphology: Geomorphological mapping and the study of submarine

landslides. In *Developments in earth surface processes* (Vol. 15, pp. 377-395). Elsevier.

Missiaen, T., Evangelinos, D., Claerhout, C., De Clercq, M., Pieters, M., & Demerre, I. (2018). Archaeological prospection of the nearshore and intertidal area using ultra-high resolution marine acoustic techniques: Results from a test study on the Belgian coast at Ostend-Raversijde. *Geoarchaeology*, *33*(3), 386-400.

Mueller, C., Woelz, S., & Kalmring, S. (2013). High-resolution 3D marine seismic investigation of Hedeby Harbour, Germany. *International Journal of Nautical Archaeology*, *42*(2), 326-336.

Müller, C., Woelz, S., Ersoy, Y., Boyce, J., Jokisch, T., Wendt, G., & Rabbel, W. (2009). Ultra-high-resolution marine 2D–3D seismic investigation of the Liman Tepe/Karantina Island archaeological site (Urla/Turkey). *Journal of Applied Geophysics*, *68*(1), 124-134.

Müller, S., & Wunderlich, J. (2003). Detection of embedded objects using parametric sub-bottom profilers. *The International hydrographic review*.

Neubauer, W. (2004). GIS in archaeology—the interface between prospection and excavation. *Archaeological Prospection*, *11*(3), 159-166.

Papadopoulos, N. (2021). Shallow offshore geophysical prospection of archaeological sites in eastern Mediterranean. *Remote Sensing*, *13*(7), 1237.

Plets, R., Dix, J., Adams, J., & Best, A. (2008). 3D reconstruction of a shallow archaeological site from high-resolution acoustic imagery: the Grace Dieu. *Applied Acoustics*, *69*(5), 399-411.

Plets, R. M., Dix, J. K., Adams, J. R., Bull, J. M., Henstock, T. J., Gutowski, M., & Best, A. I. (2009). The use of a high-resolution 3D Chirp sub-bottom profiler for the reconstruction of the shallow water archaeological site of the Grace Dieu (1439), River Hamble, UK. *Journal of Archaeological Science*, *36*(2), 408-418.

Producers, I. A. o. O. a. G. (2020). IOGP P6/11 Seismic Bin Grid Data Exchange Format. In.

Quinn, R., Breen, C., Forsythe, W., Barton, K., Rooney, S., & O'Hara, D. (2002). Integrated geophysical surveys of the French Frigate La Surveillante (1797), Bantry Bay, Co. Cork, Ireland. *Journal of Archaeological Science*, *29*(4), 413-422.

Schwardt, M., Wilken, D., & Rabbel, W. (2019). Reducing Seismic Multiples in Very Shallow Water Archaeological Prospection. 25th European Meeting of Environmental and Engineering Geophysics,

Schwardt, M., Wilken, D., & Rabbel, W. (2021). Attenuation of Seismic Multiples in Very Shallow Water: An Application in Archaeological Prospection Using Data Driven Approaches. *Remote Sensing*, *13*(10), 1871.

Shin, J., Ha, J., Chun, J.-H., & Um, I.-K. (2022). Field application of 3D CHIRP for geological surveys of shallow coastal regions. *Marine Geophysical Research*, *43*(2), 13.

Stolt, R. H. (1978). Migration by Fourier transform. *Geophysics*, *43*(1), 23-48.

Tywoky. (2022, 2022). Hafrsfjord wreck V2 - V2. https://sketchfab.com/3d-models/hafrsfjord-wreck-v2-5da5f11481424ada9bf0e358b6e8fc02

Wilken, D., Hadler, H., Wunderlich, T., Majchczack, B., Schwardt, M., Fediuk, A., Fischer, P., Willershäuser, T., Klooß, S., & Vött, A. (2022). Lost in the North Sea—Geophysical and geoarchaeological prospection of the Rungholt medieval dyke system (North Frisia, Germany). *Plos one*, *17*(4), e0265463.

Wilken, D., Wunderlich, T., Hollmann, H., Schwardt, M., Rabbel, W., Mohr, C., Schulte-Kortnack, D., Nakoinz, O., Enzmann, J., & Jürgens, F. (2019). Imaging a medieval shipwreck with the new PingPong 3D marine reflection seismic system. *Archaeological Prospection*, *26*(3), 211-223.

Wilkinson, T. J., & Murphy, P. (1986). Archaeological survey of an intertidal zone: the submerged landscape of the Essex coast, England. *Journal of Field Archaeology*, *13*(2), 177-194.

Winton, T. (2019). Quantifying depth of burial and composition of shallow buried archaeological material: integrated sub-bottom profiling and 3D survey approaches. *3D Recording and Interpretation for Maritime Archaeology*, 155-174.

Wunderlich, J., Wendt, G., & Müller, S. (2005). High-resolution echo-sounding and detection of embedded archaeological objects with nonlinear sub-bottom profilers. *Marine Geophysical Research*, *26*(2-4), 123.

XSGeo. (1999). SEISMIC ACQUISITION. http://xsgeo.com/acq.htm

Yilmaz, Ö. (2001). *Seismic data analysis: Processing, inversion, and interpretation of seismic data*. Society of exploration geophysicists.